НИУ «Московский Энергетический Институт (ТУ)»

Кафедра Теоретической Механики и Мехатроники

Библиографический обзор

по теме НИР:

«Исследование методов искусственного интеллекта в групповом управлении роботами»

Выполнил: ст. гр. С-11-07 Дедков В.А.

Научный руководитель: профессор Кирсанов М.Н.

Москва 2012

1. Кирсанов М.Н. Графы в Maple. Задачи, алгоритмы, программы. — М.: Издательство ФИЗМАТЛИТ, 2007. — 168 с. — ISBN 5-7046-1168-0.

Основной источник при написании программы.

Из книги были взяты методы, описанные при решении задачи коммивояжера (глава 4.8).

Муравьиный алгоритм Марко Дориго.

Функция, управляющая переходом из данной вершины i в вершину j , k — номер муравья, движущегося по дугам графа:

$$P_{ij,k} = \frac{\tau_{ij}^{\alpha}\eta_{ij}^{\beta}}{\sum_m \tau_{im}^{\alpha}\eta_{im}^{\beta}},$$

где τ_{ij} — количество феромона, оставленного роботом на дуге $[i, j]$; η_{ij}— величина, обратная весу (длине) дуги $[i, j]$; α, β — эмпирические коэффициенты.

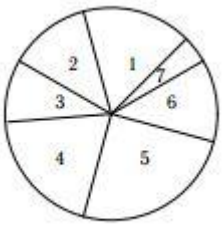

Рис. 4.58

Пусть муравей k подошел к некоторой вершине 8 и обнаружил, что перед ним 7 возможных путей к семи вершинам (на уже пройденные он внимания не обращает). Куда идти? Муравей доверяется случаю. Он «пускает рулетку» (рис. 4.58).

Алгоритм имитации отжига.

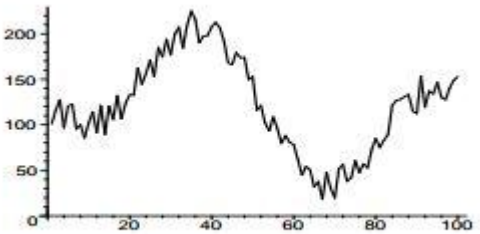

Рис. 4.59

Если полученный маршрут лучше всех существовавших ранее, то этот маршрут берется за очередной. Если маршрут хуже, то самый простой вариант — это не брать его (зачем ухудшать решение?). Однако так решение может закатиться в один из локальных минимумов, которыми изобилуют подобные задачи (рис. 4.59).

Вероятность выбора худшего решения:

$$P = exp(-\Delta L/T)$$

где ΔL — положительная разность между качеством тестируемого и

ранее полученного оптимального решений, T — некоторый постоянно уменьшающийся параметр (условно — температура).

Снижение температуры обычно производится по формуле $T_{k+1} = \alpha T_k$, где $0 < \alpha < 1$.

2. Turk J Elec Engin, VOL.15, NO.2 2007, TUBITAK - A Review of Studies in Swarm Robotics - Levent BAYINDIR and Erol SAHIN

В статье авторы классифицировали проблемы групповой робототехники и исследования в данной области.

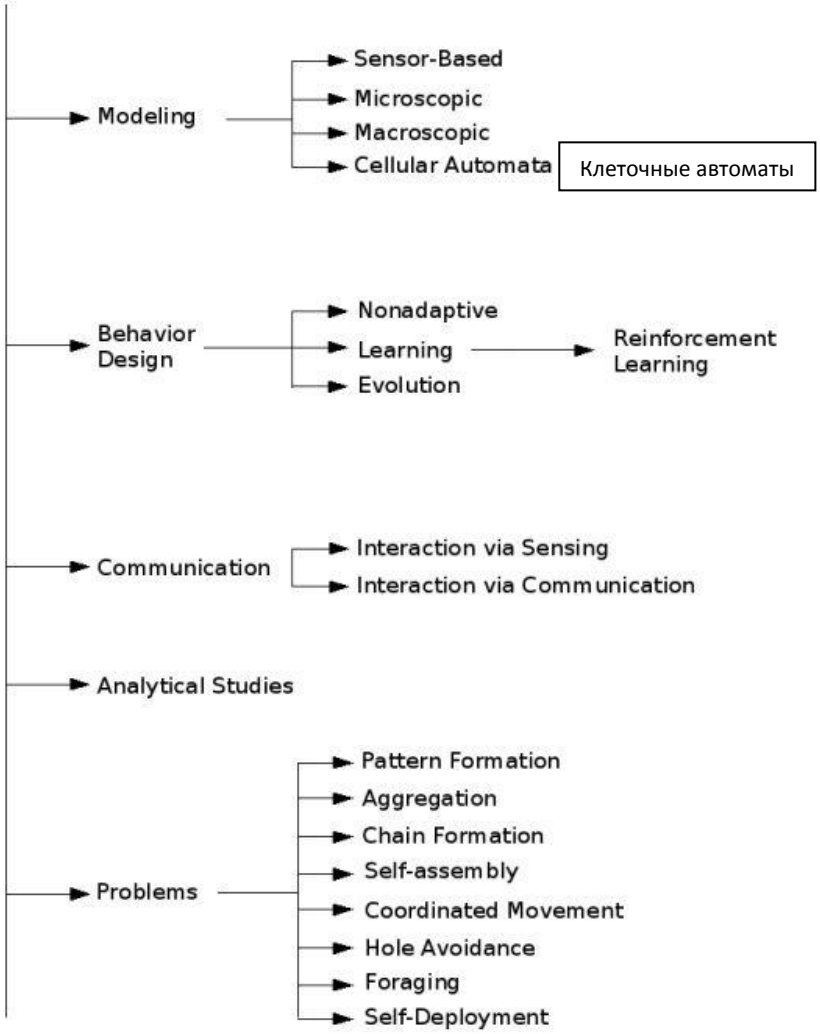

Figure 1. Taxonomy of Swarm Robotics Literature. The taxonomy is divided into five main axes namely modeling, behavior design, communication, analytical studies and problems.

Классификация исследований по групповой робототехнике. 5 основных областей: построение моделей исследований, моделирование поведения роботов, взаимодействие роботов, аналитические исследования и проблематика.

3. Donald Miner – University of Maryland, Baltimore County – 2007 [class paper] "Swarm Robotics Algorithms: A Survey" (pdf) ~ CMSC 677 - Agent Architectures and Multi-agent Systems

В статье рассматриваются 6 алгоритмов управления группами роботов (6 задач и решений в группах роботов), дается краткий обзор современного состояния данной области исследований. Приведенные эксперименты показывают, что данные алгоритмы масштабируемы, устойчивы к ошибкам и эффективны.

Все приведенные алгоритмы испытывались в реальных группах роботов на проектах The iRobot Swarm и Swarm-bots project (координатор Марко Дориго).

1. Dispersion in Indoor Environments (Задача равномерного распределения в закрытом помещении)

Figure 6: *The iRobot swarm uniformly dispersed over a somewhat complex environment (left) and an open space (right).*

Решение: отталкивание от C ближайших соседей. Эксперименты показывают, что лучшие результаты при $C = 2$.

2. Distributed Localization and Mapping (Задача распределенного размещения и составления карты)

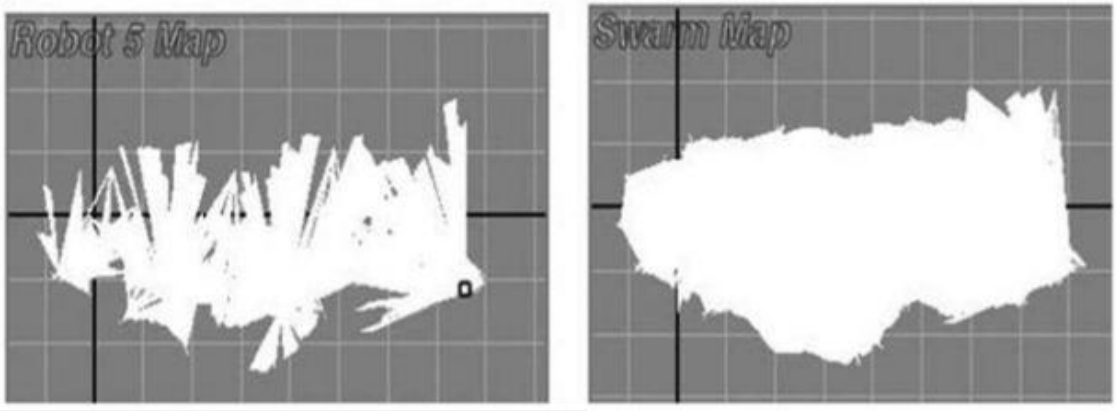

Figure 7: *A visualization of the distributed mapping algorithm. The left image shows the map contribution of a single robot. The right image shows all the robots' personal maps superimposed on one another.*

Решение:

1. Move in a general direction while maintaining a X, Y coordinate based on local beacons (маяки).

2. If the number of beacons goes below a certain threshold, become a beacon and start broad-casting position information to others.

3. If the number of dependent modules goes below a certain threshold, stop being a beacon and return to step 1.

3. Mobile Formations (Задача перемещения локальной группы роботов к цели через группу препятствий)

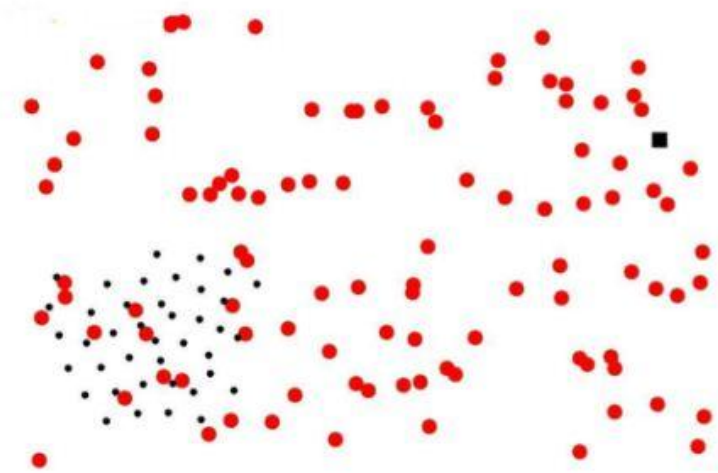

Figure 8: *A visualization of forty robots (small black dots) going towards a goal (black square). They must avoid obstacles (large red dots) while still maintaining a tight formation.*

4. Cooperative Hole Avoidance (Задача коллективного объезда ям)

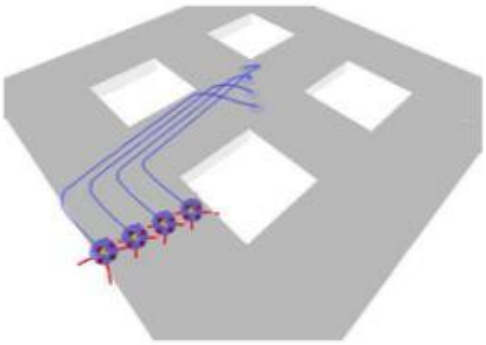

Figure 9: *Four connected S-bots moving through a hole riddled environment.*

(riddle – решето, сеять)

5. Chain Based Path Formation (Задача формирования цепи между «гнездом» и «добычей»)

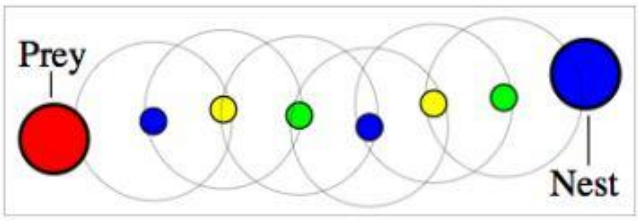

Figure 10: *A visualization of S-bots (small colored circles) forming a chain from a "nest" to a "prey." Each S-bot must be able to see (range given by thin grey circle) other s-bots in the chain.*

(nest - гнездо, prey - добыча)

Figure 11: *A picture of S-bots forming a chain from the nest to the prey.*

6. Group Transport (Задача групповой транспортировки)

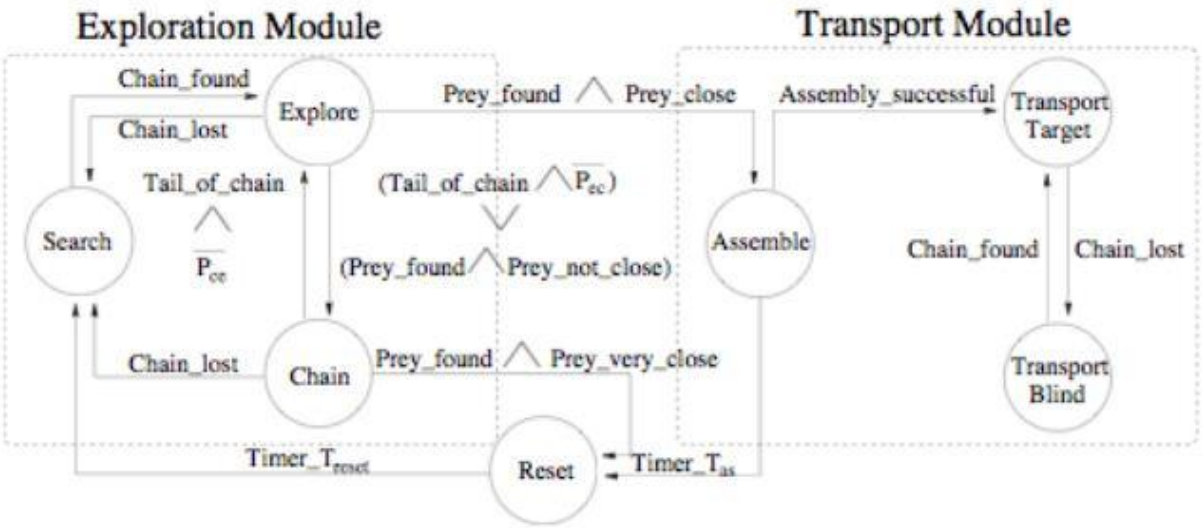

Figure 12: *The state diagram of the control program of each S-bot for this algorithm.*

Figure 13: *A picture of S-bots dragging the prey to the nest.*

4. P. Valdastri, P. Corradi, A. Menciassi, T. Schmickl, K. Crailsheim, J. Seyfried, P. Dario, "Micromanipulation, Communication, Swarm Intelligence Issues in a Swarm Microrobotic Platform," Robotics and Autonomous Systems, 54 (2006) 789-804.

В статье описывается новая платформа (программа) для исследования групп микророботов с целью применения роевого интеллекта на практике.

Рассматривается моделирование группы микророботов, у которых стоит задача собрать всю пыль из двух областей и переместить её в пылесборник (3я область).

Ограничения роботов:

1. Робот обнаруживает пыль или пылесборник, только если он непосредственно находится в этих областях («стоит» на них).

2. Роботы взаимодействуют друг с другом посредством светодиодов на расстоянии 3-4 собственных диаметров.

Оптимальное поведение роботов (с учётом ограничений):

1. Использование «от робота к роботу» коммуникации, для того, чтобы определить положение целевых областей.

2. Роботы должны использовать всё преимущество большого размера роя для локализации областей.

3. Робот может потерять частицу пыли, поэтому оптимальный вариант движения к пылесборнику по кратчайшему расстоянию.

Для моделирования использовалась программа LaRoSim V0.42, выполненная на NetLogo 3.02.

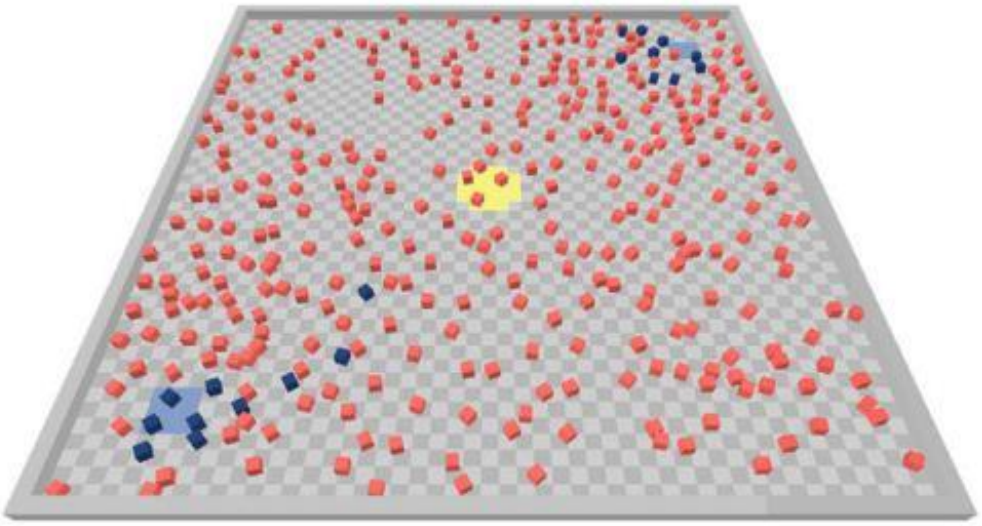

Fig. 12. A screenshot of the LaRoSim simulation platform. The screenshot shows the typical "cleaning"-scenario simulated within this platform: The two blue-coloured floor areas represent "dusty" areas that have to be cleaned by the robot swarm autonomously. Empty robots (red boxes) head towards these areas. As soon as they pick up a dust particle they are coloured in blue. These loaded robots then head towards the yellow dump area to drop the particle there. (For interpretation of the references to colour in this figure legend, the reader is referred to the web version of this article.)

Синие области – области с пылью, желтая область – пылесборник, синие роботы – роботы с частицами пыли.

Для определения направления движения, роботы используют стратегию сообщения, основанную на векторах (The "vector-based" communication strategy).

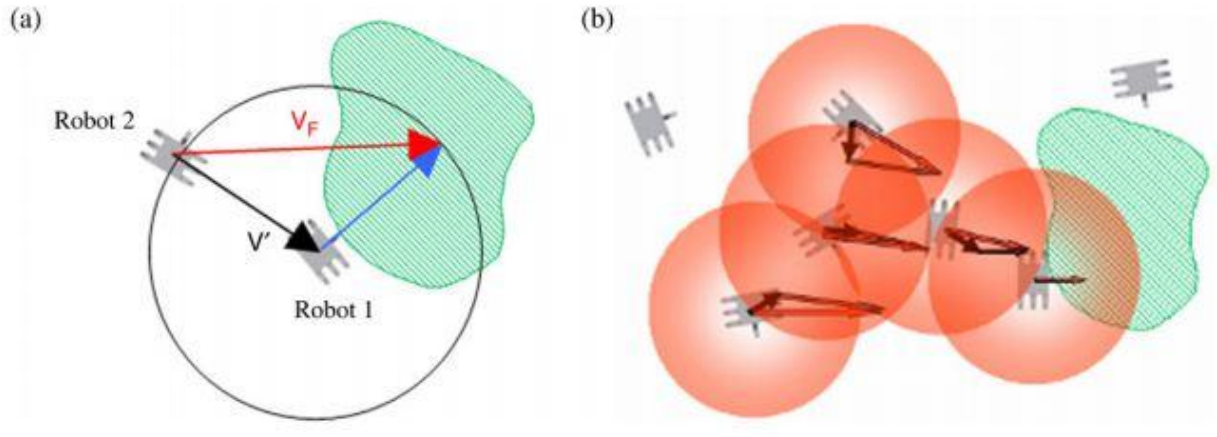

Fig. 13. (a) Vectorial sum for target direction reconstruction. (b) An example of the swarm formation induced by vector propagation within a group of 5 robots.

Основные настройки программы (с учётом ограничений возможностей предполагаемой аппаратуры)

Table 1
Default parameter settings used in the simulation experiments described in this article

Parameter	Value
Arena-size	49 × 49 rd
Dust-particles	72 particles
Robot-speed	0.5 rd/step
Error-distance-measure	10%
Error-in-communication	10%
Communication-radius	3.5 rd
Number-of-LEDs	4
Inter-LED-angle	90°
LED-beam-aperture	60°
P (communication-break)	0.1
Communication-capacity	32 bit/message
Dust-in-arena	72 particles

This table gives only those parameters that reflect hardware constraints and arena features. The strategy-parameters, that are shaped by artificial evolution, are described separately. The unit "rd" represents the maximum diameter of one robot.

Ввод отрицательных обратных связей и обновление информации в системе

В природе в коллективном поведении присутствует отрицательная обратная связь (пример – испарение феромона у муравьев), в программе тоже вводится отрицательная обратная связь.

(1) Use-hop-count: использовать ли счётчик переходов для каждого вектора (инкремент, когда новая связь устанавливается). Предотвращает «разрастание» старой информации о связях в системе. TRUE или FALSE.

(2) p(vector-forget): вероятность стирания информации о векторах из памяти робота. Срабатывает на каждом шаге робота. $[0, 1]$

(3) Is-Scout: является ли робот разведчиком. Если является, то робот не использует информацию о векторах (указывающих на области с пылью или пылесборник), как следствие, такие роботы не собираются в одном месте и постоянно блуждают, передавая информацию другим роботам. TRUE или FALSE.

(4) "weight-find-dust" и "weight-find-dump" – вероятность следования направлению вектора. $[0, 1]$

Результаты

Для формирования роя использовался генетический алгоритм. Всего формировалось 120 поколений роев. В каждом поколении 10 роев.

Для оценки качества роя была использована fitness-функция: 40 очков за доставку частицы пыли в пылесборник, 20 за нахождение частицы пыли, но в дальнейшем частица терялась. За каждое уменьшение пути 10 очков.

Экстремальные значения fitness-функции:

2860 очков: ниже этого значения каждый рой неудачный – не были доставлены все частицы пыли.

8360 очков: самое высокое значение fitness-функции. Было достигнуто за 250 шагов (наименьшее время работы программы).

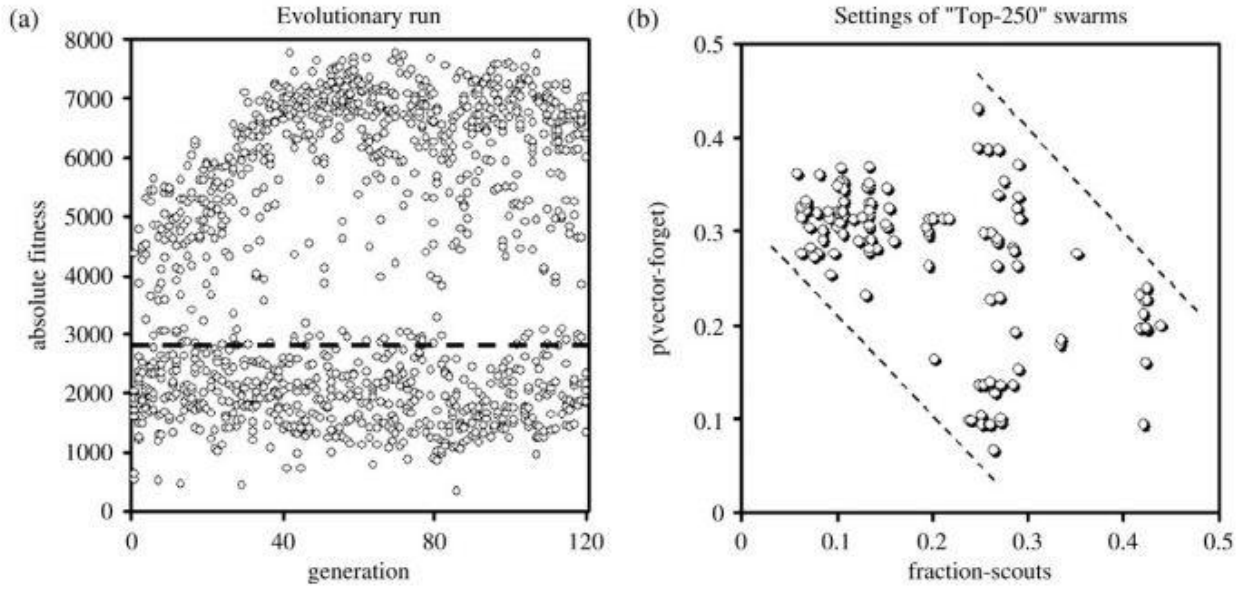

Fig. 14. (a) Results of the "Evolutionary Strategy". Throughout 120 generations, more-and-more effective swarms evolved, what is expressed by the absolute fitness. The dashed line indicates the maximum amount of fitness points a swarm can achieve without removing all dust particles in the arena. In total, 1200 simulation runs are depicted in the left subfigure. (b) Two related parameters, p(vector-forget) and fraction-scouts, that evolved in specific combinations. This subfigure shows the 250 fittest swarms that evolved between generations 35 and 100 (the "plateau" in the left subfigure). The two dashed lines indicate that the 250 best swarms show a negative correlation between these two parameters. Two swarms at the extremes of these settings are depicted in Fig. 16 at runtime.

Двум экстремальным значениям на рис. 14(b) соответствует следующее расположение роботов на рис. 16.

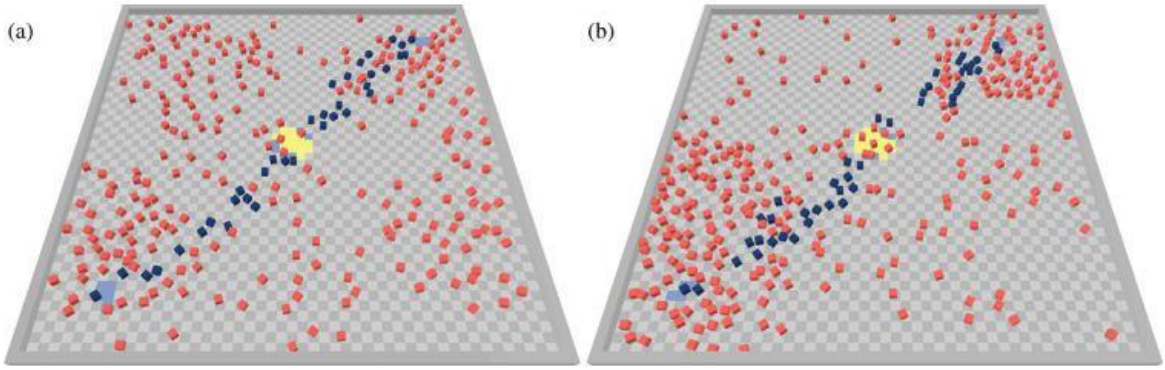

Fig. 16. (a) Screenshot of one type of very fit swarms. This type (type 1) has a low fraction of scouts in the swarm (8%) and a high p(vector-forget)=0.29. (b) A screenshot of the other type of very fit swarms. This type (type 2) has a high scout-to-worker ratio (27%) and a low value of p(vector-forget)=0.14. These different parameter settings result in different global behaviour but in the same swarm efficiency, as it was measured by our fitness function. The swarm in the right figure shows a more intensive aggregation of empty robots around the dust areas, the left swarm builds several "sub-swarms" that are narrowly connected.

Table 2
The parameters that evolved during our Evolutionary Strategy

Parameter	Type 1:	Type 2:
Absolute fitness	7771 points	7766 points
Density-of-robots	11.8%	13.2%
Fraction-scouts	8%	27%
p(vector-forget)	0.29	14%
Use-hop-count	true	true
Priority-coll-avoid-dist	0.4 sr	0.41 sr
Empty-coll-avoid-dist	0.65 sr	0.77 sr
Loaded-coll-avoid-dist	0.25 sr	0.27 sr
Priority-signal-scouts	FALSE	FALSE
Priority-signal-loaded	TRUE	TRUE
Weight-find-dust	0.83	0.82
Weight-find-dump	0.94	1.00

The table shows the parameter settings of the two swarm types that are displayed in Fig. 16. The unit "sr" refers to the sensory radius of the robots, which was set to 3.5 rd (robot diameters).

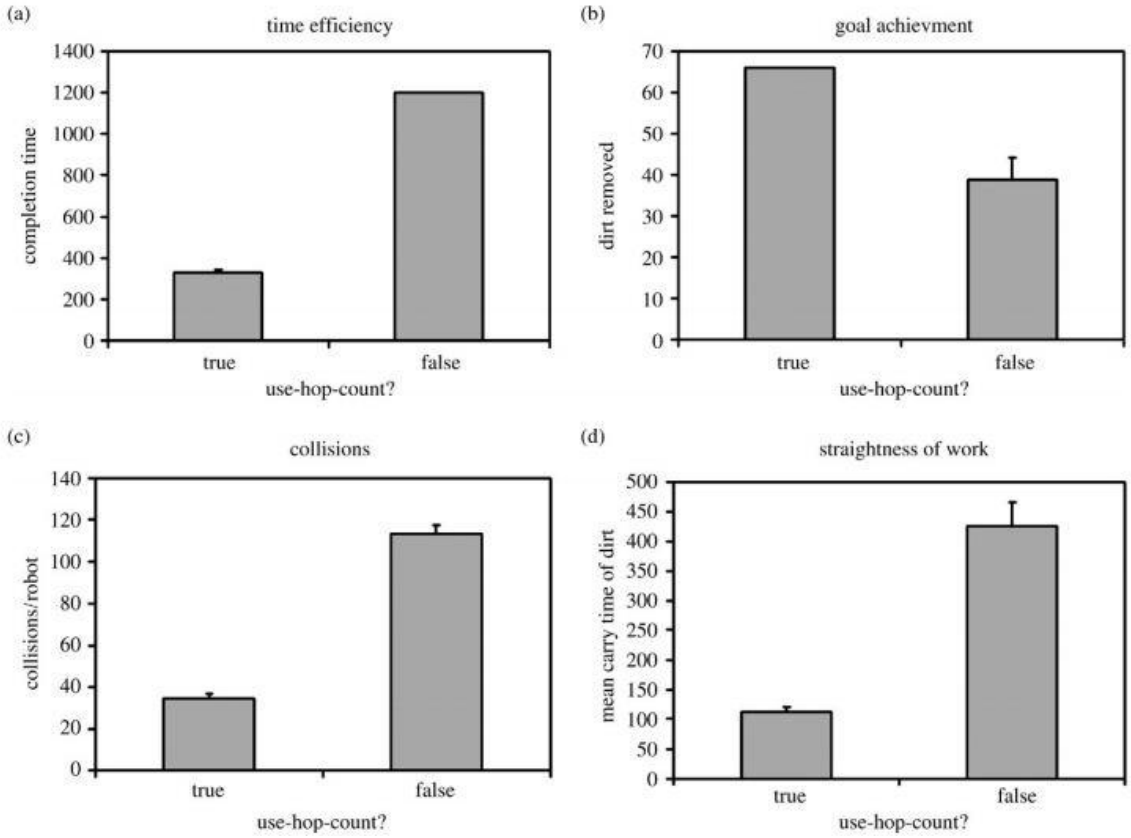

Fig. 15. The importance of the parameter "use-hop-count" for the vector-based strategy. If this parameter is set to TRUE, than the goal is achieved much more quickly (a), more dust is removed (b), fewer collisions happen (c) and the dust particles are carried on a shorter way to the dump area (d). All figures show medians and third quartiles. N = 12 per setting (per bar).

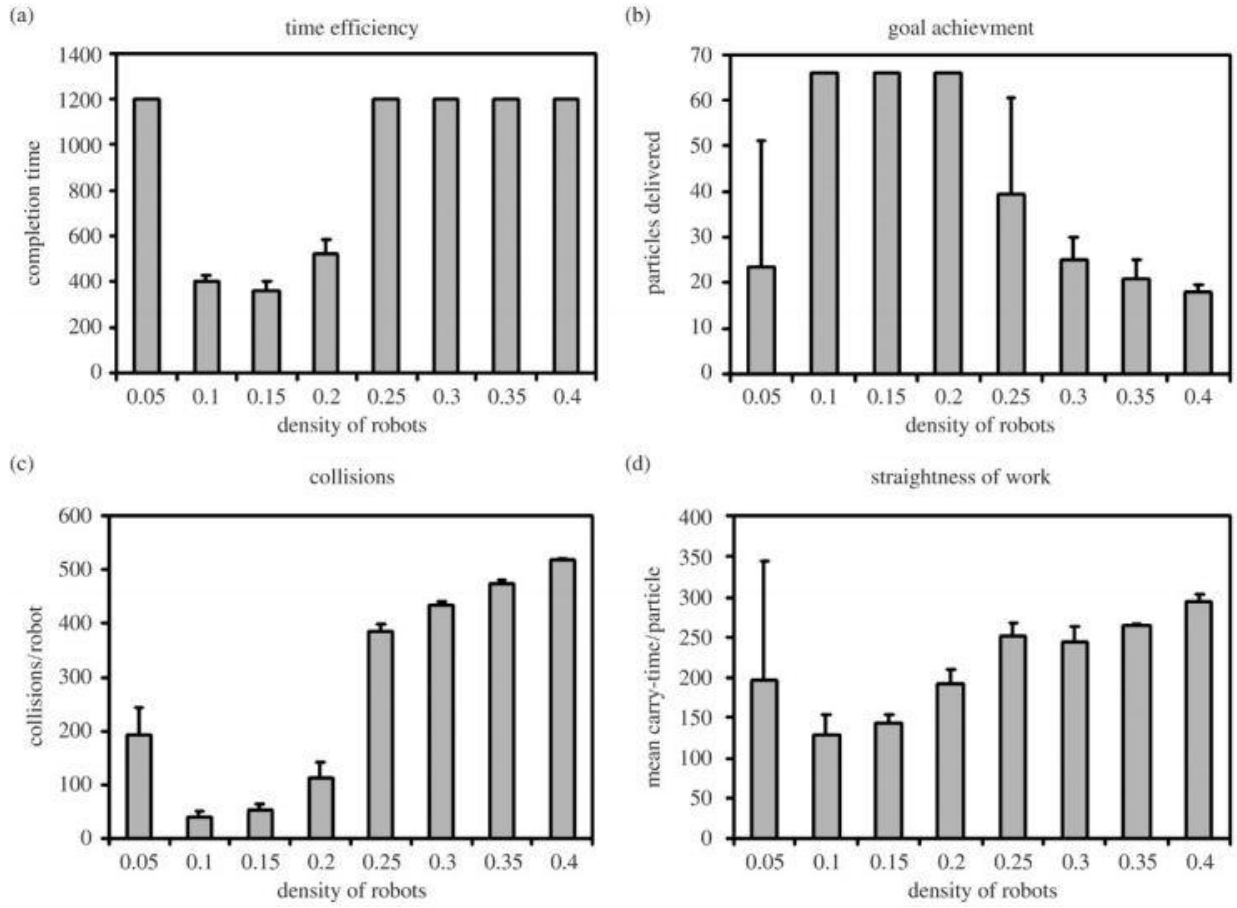

Fig. 17. The optimal density of the robot swarm is evaluated. (a) With a density between 0.1 and 0.15, the swarms finished their work in the shortest period. (b) Swarm densities between 0.1 and 0.2 allowed successful cleaning of the whole arena. (c) Swarms with densities between 0.1 and 0.15 showed the lowest collision rate per robot. (d) Densities between 0.1 and 0.15 led to the lowest mean carriage periods per dust particle. All figures show medians and third quartiles. N = 6 per setting (per bar).

5. Schmickl, Thomas; Thenius, Ronald; Moeslinger, Christoph; Radspieler, Gerald; Kernbach, Sergej; Szymanski, Marc; Crailsheim, Karl; "Get in touch: cooperative decision making based on robot-to-robot collisions". In: Autonomous Agents and Multi-Agent Systems (2008), 1 - 23.

В статье исследуется реальная группа роботов, моделирующих поведение новорожденных рабочих пчел на плоскости с разными температурными зонами.

Известно, что пчёлы при выборе места следуют температурным предпочтениям, и выбирают для себя наиболее комфортную температуру. Для новорожденных рабочих пчёл эта температура 34 – 38 град. по Цельсию. Единственная пчела будет двигаться по плоскости с различными температурными областями почти случайным образом (чаще выбирая более тёплое место). Но группа из 15 пчёл будет устойчиво формировать кластеры в тёплой области.

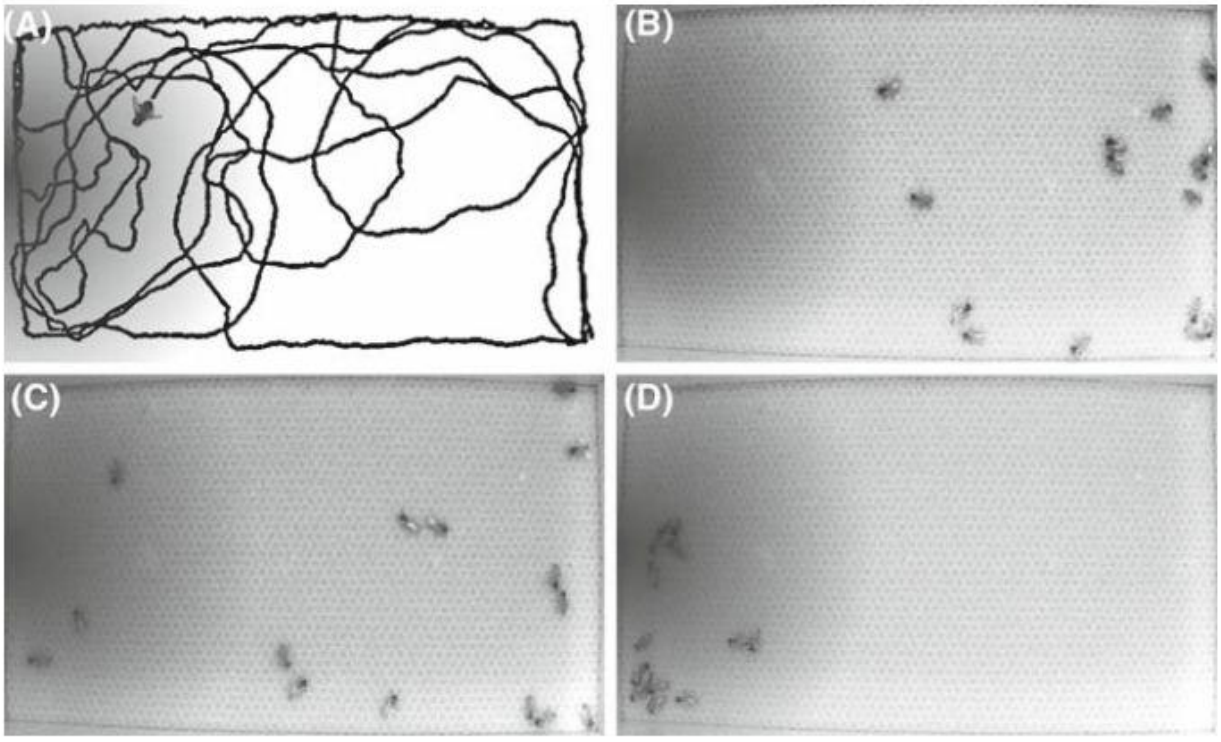

Fig. 1 Navigation behaviour of young bees (1 day old) in a temperature gradient. All figures: The warm area (approx. 38°C) is on the left side of the arena, as indicated by the dark spot. The right side of the arena had a temperature of 31°C. Young honeybees prefer temperature between 34°C and 38°C [9]. (**a**) Trajectory of one single bee for 8 min. (**b–d**) Time lapse of the same experiment with 15 bees (30 s, 1 min, and 10 min after the release of the bees in the arena). Bees were released in the colder area on the right side of the arena

Исходя из такого поведения пчёл, был предложен алгоритм коллективного поведения группы роботов, названный BEECLUST.

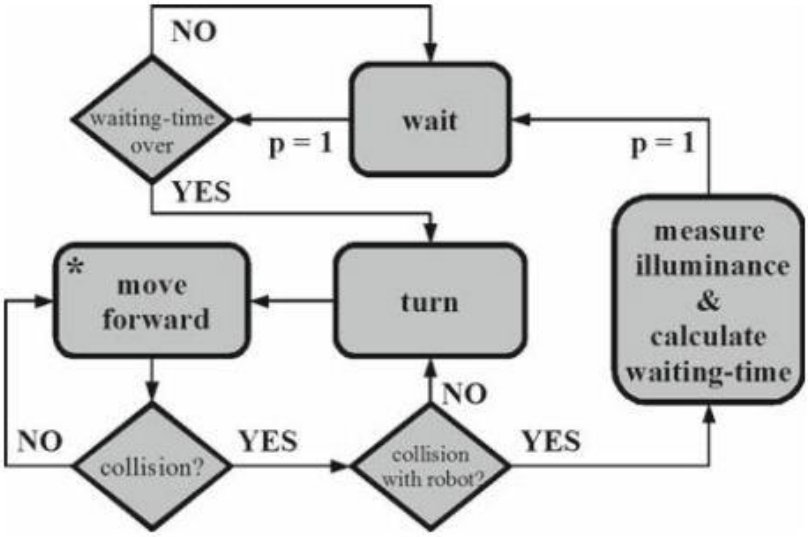

Fig. 2 State-diagram of our control algorithm BEECLUST. Rounded boxes represent behavioural states of a robot, diamonds identify control structures (if-else) and arrows indicate state transitions. Texts at the arrows indicate probabilities of these transitions (p-values) or events that trigger a transition

1. All robots move randomly in the arena. Whenever a robot detects an obstacle in front, it stops and listens for possible collision-avoidance signals. If such signals are detected, the robot assumes that the obstacle is another robot. If no such signals are detected, the robot assumes that the obstacle is a wall.

2. After a robot encounters a non-robotic obstacle, it turns randomly and continues with step 1.

3. After a robot encounters another robot, it stops and measures the local illuminance.

4. The higher the local illuminance, the longer the robot waits on the place. After the robot has finished its waiting term, it rotates randomly and proceeds with step 1.

Исследования проводились в группе роботов, реагирующих на свет.

Проводились 2 вида исследований:

1. При статичном освещении.

2. При динамичном освещении.

Исследования проводились на 3 типах освещения:

1. Нет света.

2. Тусклый свет.

3. Яркий свет.

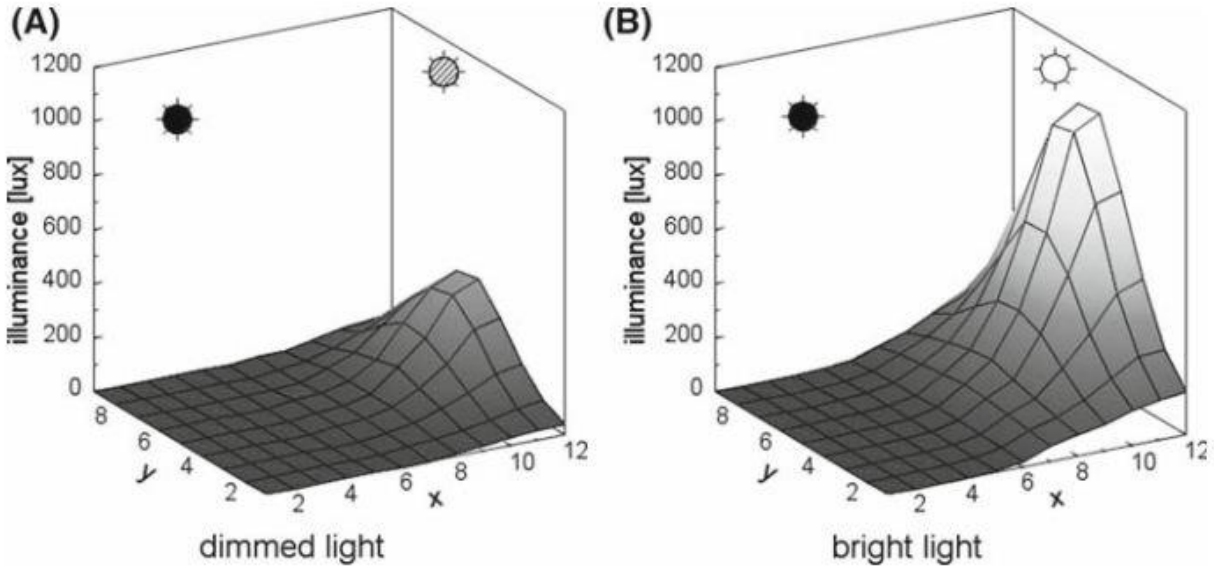

Fig. 5 Spatial distribution of illuminance in the arena during the two experiments that focussed on the collective behaviour of the robotic swarm in a static environment. (**a**) Spatial distribution of illuminance within the arena with one dimmed light (390 lux). (**b**) Spatial distribution of illuminance within the arena with one bright light (1,100 lux). The third setup with no light in the arena is not shown in the figure. The small sun-like symbols in the upper sections of the graphs represent the lights' intensities at the respective side. A striped sun indicates that the light was dimmed; a white sun indicates that the light was bright and the black sun indicates that the light was switched off

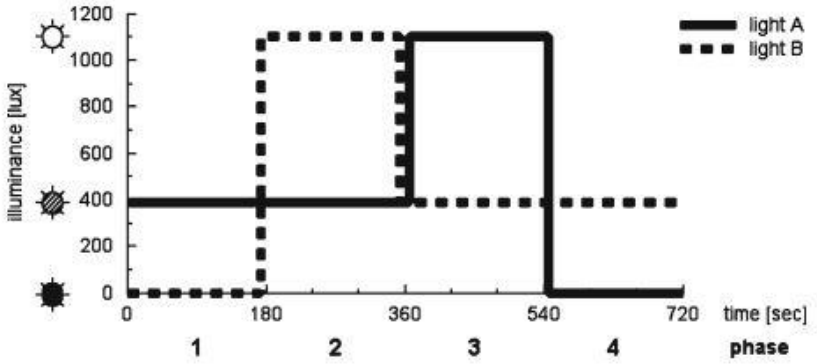

Fig. 6 Timing of our experiments focussing on the behaviour of the robotic swarm in a dynamic environment. Every 180 s the lights' intensities were modified, thus changing the environmental conditions for the robotic swarm

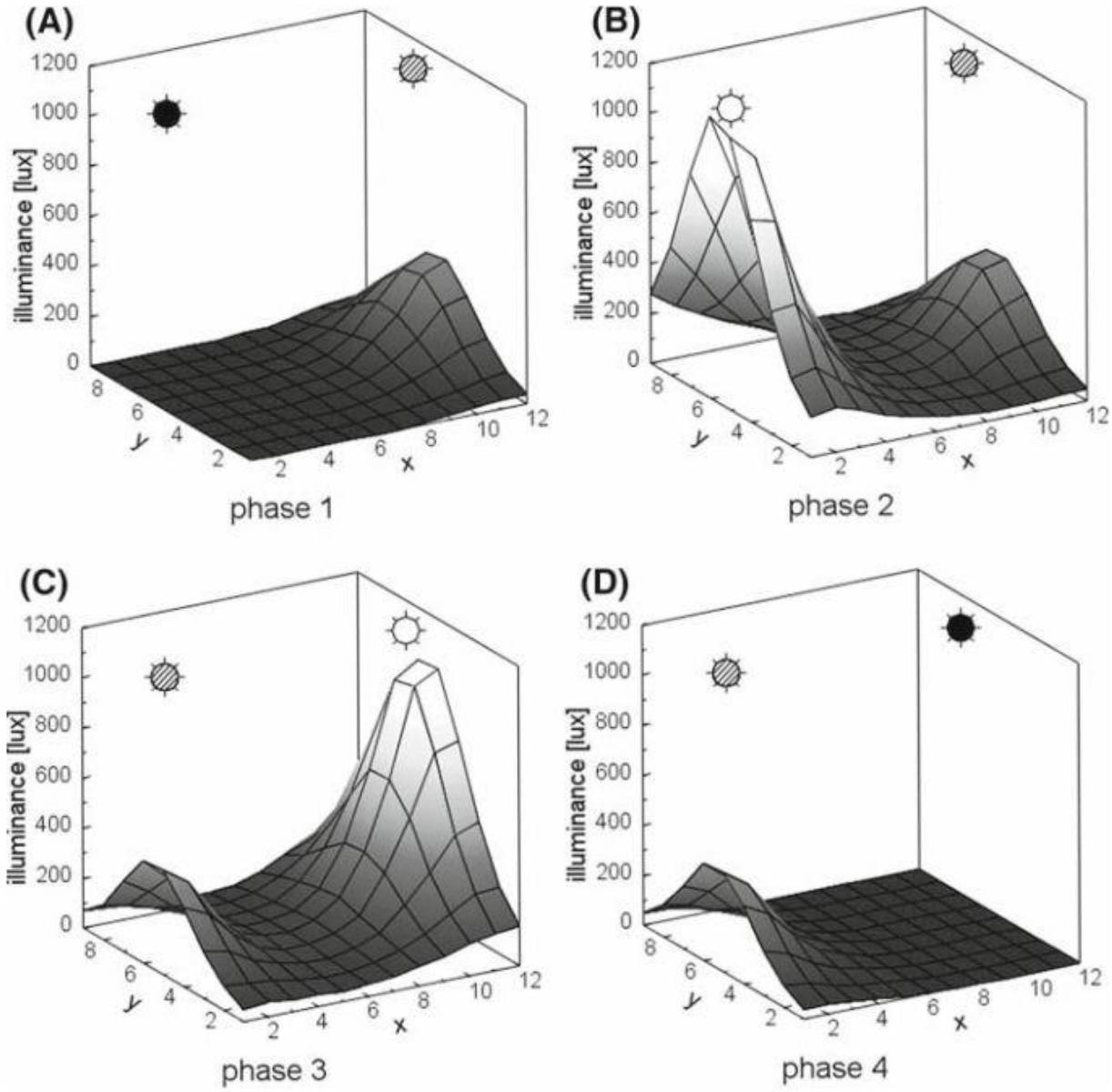

Fig. 7 Spatial distribution of illuminance in the arena during the four distinct phases of our experiments in the dynamic environment. The small sun-like symbols in the upper sections of the graphs represent the lights' intensities at the respective light. A striped sun indicates that the light was dimmed; a white sun indicates that the light was bright and the black sun indicates that the light was switched off

Кроме того, освещенные зоны делились на 4 локальные зоны, в зависимости от удаления от центра (самого яркого места).

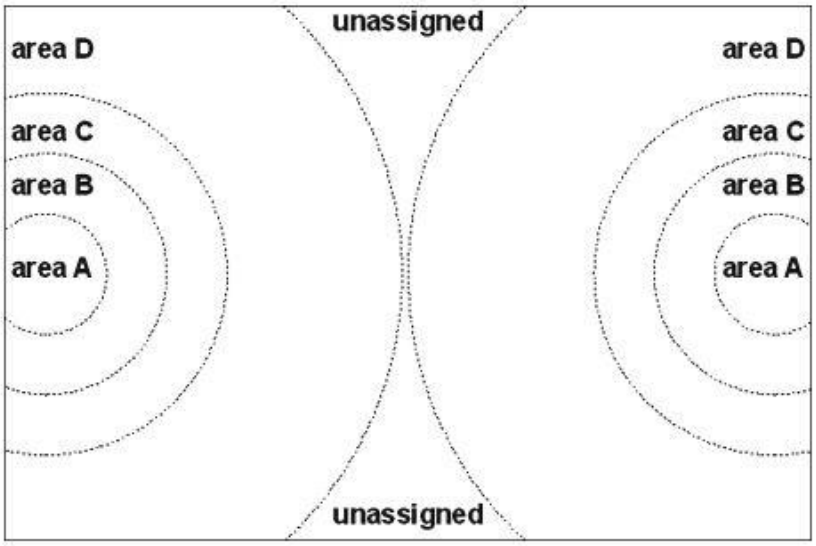

Fig. 4 Sketch of the four different areas that were used to classify how close each aggregated robot had approached the spot with the highest illuminance below the corresponding light

Table 1 Radii of the areas measured from the point of maximum illuminance

Area	Radius
A	$r < 11\,\text{cm}$
B	$11 \leq r < 22\,\text{cm}$
C	$22 \leq r < 33\,\text{cm}$
D	$33 \leq r < 66\,\text{cm}$

Функция, отображающая измеренную освещенность на время ожидания робота, после того, как он встретит другого робота – коллизия «робот-робот» (ключевое свойство алгоритма, которое управляет коллективным поведением роботов).

$$w(t) = w_{\max} \cdot \frac{s(t)^2}{s(t)^2 + \theta}$$

The variable $w(t)$represents the waiting-time of a robot in seconds, and the variable $s(t)$represents the sensor value reported by the light-sensor mounted atop the robot (for more detail see Sect.2.4). The parameter w_{max}expresses the maximum waiting time of a robot at locations of maximum (infinite) luminance. The parameter θ models the steepness of the stimulus-response curve, that his how "fast" the waiting time increases with increasing luminance in the steep part of the sigmoid curve.

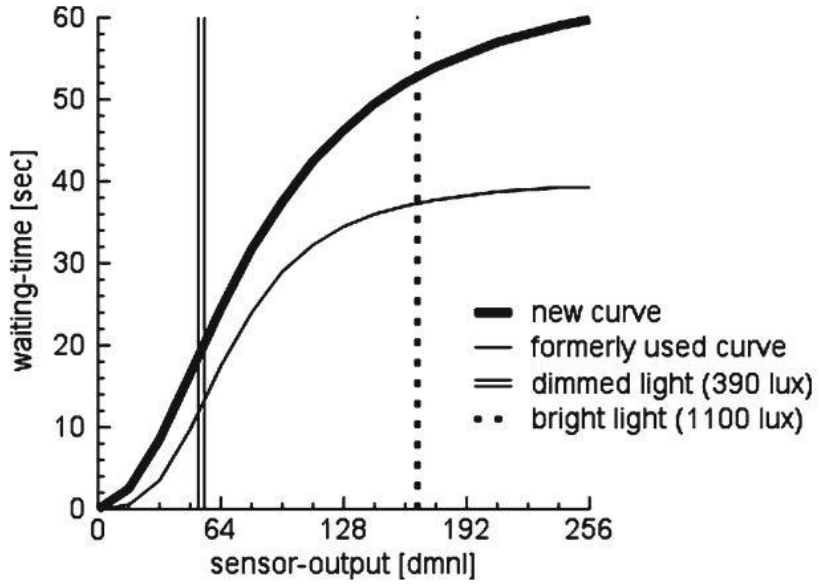

Fig. 8 Dependency of the duration of the state *"wait"* on the local illuminance measured by the robot. The bold curve indicates the function used in the experiments described in this article, the thin curve depicts the function used in [26]. The dotted vertical line indicates the median illuminance measured by the robots directly below a bright light; the vertical parallel line indicates the medium illuminance measured by the robots directly below a dimmed light

Результаты

Статическая среда

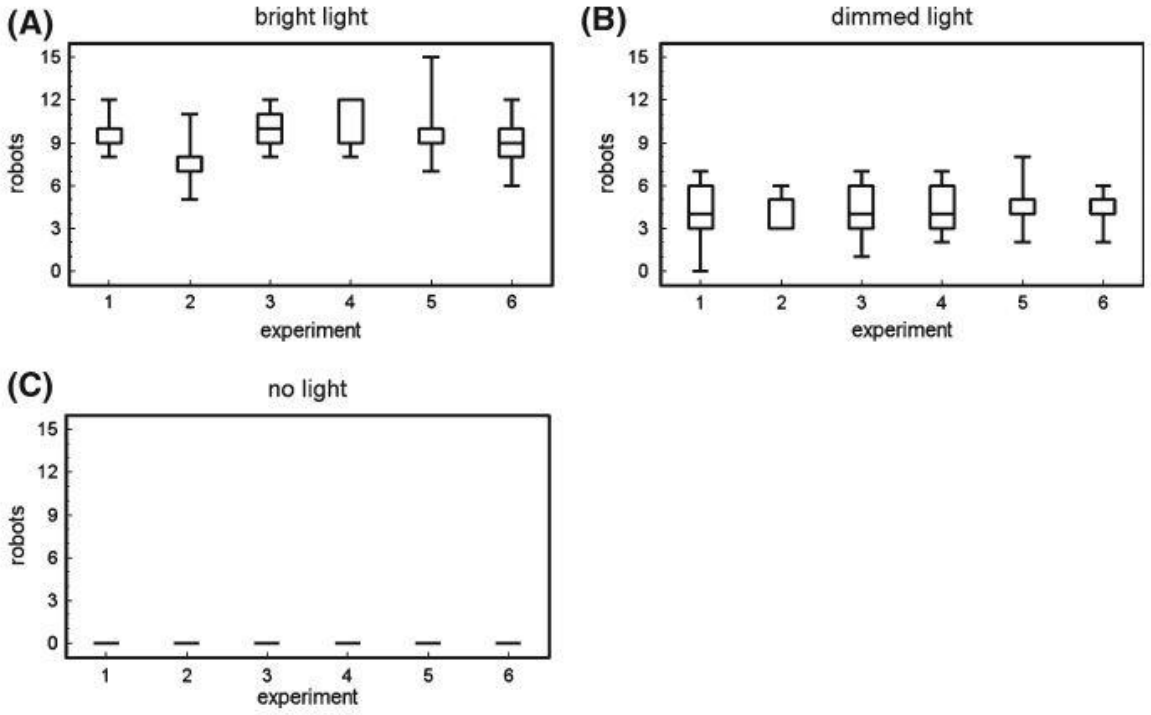

Fig. 11 (**a**) Number of aggregated robots per interval in a static environment with one bright light (1,100 lux) in the arena. Approx. 60% of all robots aggregated under this environmental condition. (**b**) Number of aggregated robots per interval in a static environment with one dimmed light (390 lux) in the arena. Approx. 30% of all robots aggregated under this environmental condition. (**c**) Number of aggregated robots per interval in a static environment without any light source. This environmental condition always resulted in no aggregation of robots. Medians, quartiles, and extremes are depicted. $N = 6$ repetitions with nine sampling intervals each

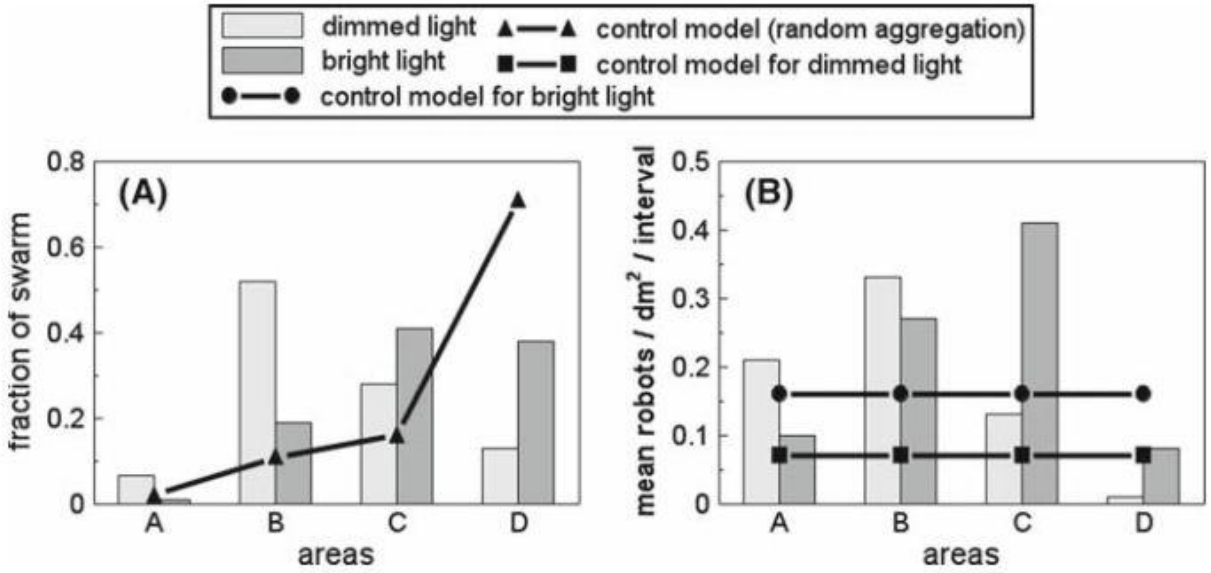

Fig. 12 (**a**) Allocation of all aggregated robots to the four areas. Bars indicate the fractions of all aggregated robots measured during our experiments with either a dimmed light or a bright light. The line indicates the numbers of aggregated robots predicted by a model of random-walk and random aggregation. (**b**) Mean number of robots per measured interval, normalized according to the different area sizes. Bars indicate the mean of the number of robots observed in the corresponding area during our experiments with either a dimmed light or a bright light. Lines indicate the number of aggregated robots predicted by a model of random-walk and of equivalent mean waiting times as was measured in the real robots for each light condition. $N = 6$ repetitions with nine sampling intervals each

Динамическая среда

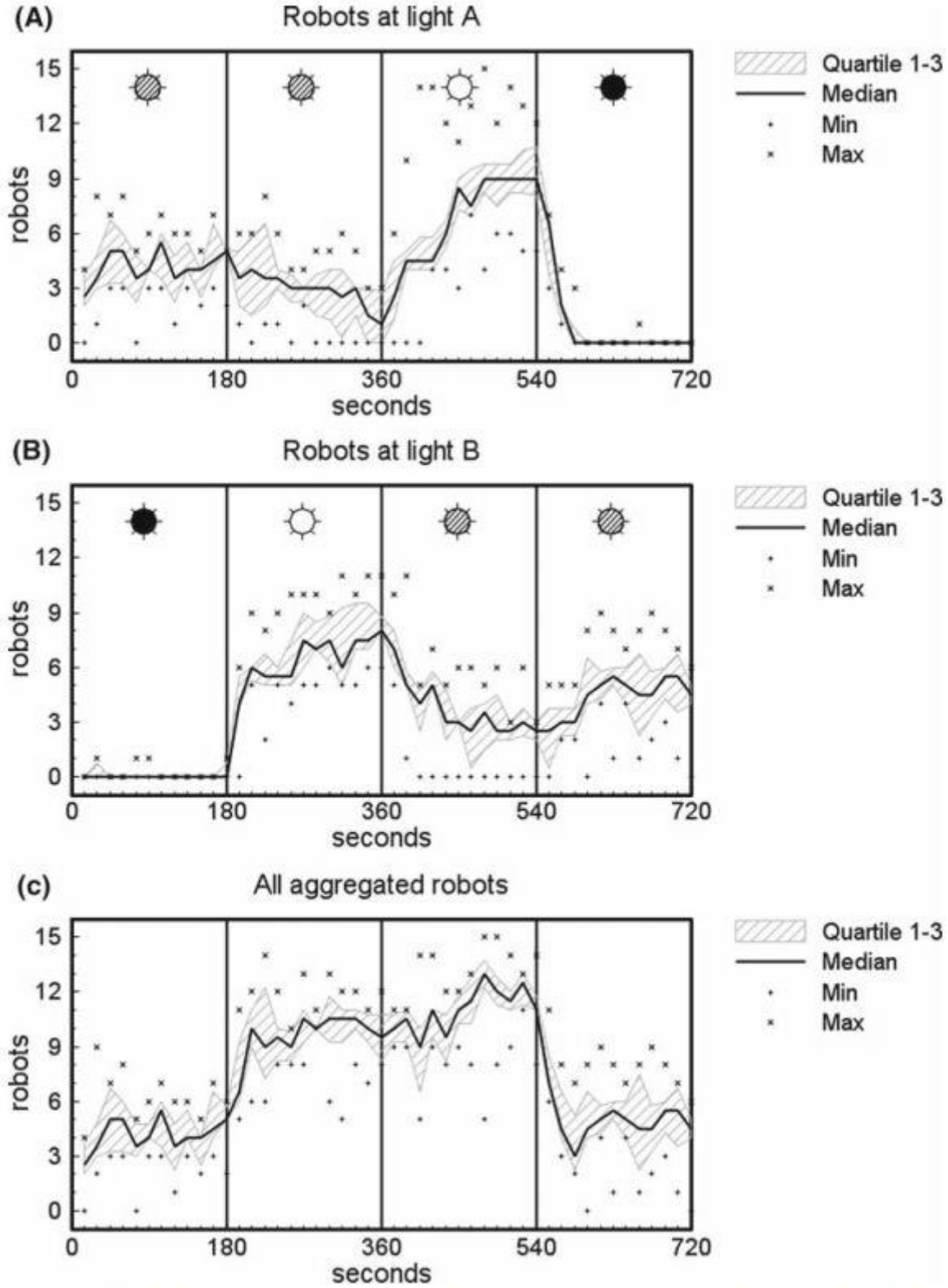

Fig. 14 (**a**) Number of aggregated robots at light A. The three vertical lines indicate the timings of the changes in the environment. (**b**) Number of aggregated robots at light B. (**c**) Total number of aggregated robots, regardless of arena side. $N = 6$ repetitions. The small sun-like symbols in the upper sections of the graphs represent the lights' intensities at the respective light. A striped sun indicates that the light was dimmed during this phase; a white sun indicates that the light was bright and the black sun indicates that the light was switched off

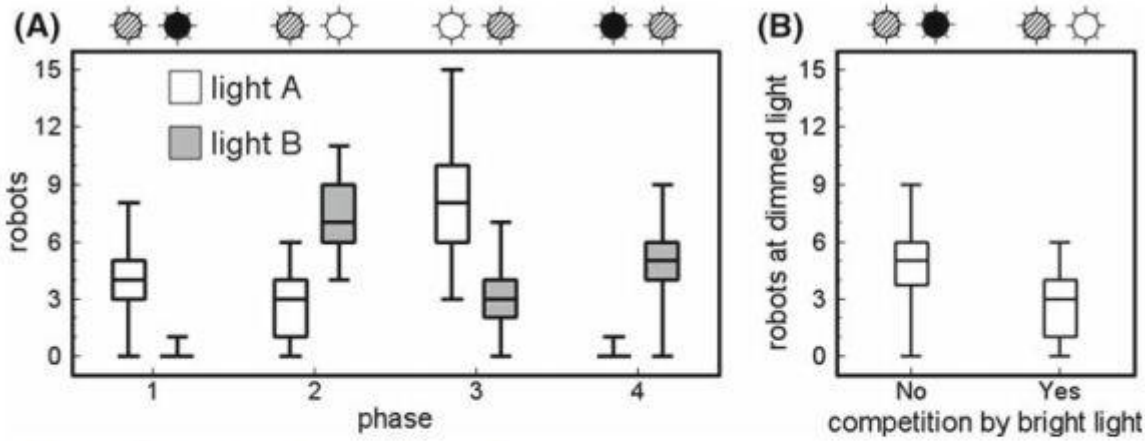

Fig. 15 (**a**) Box & whisker diagram depicting the median number of aggregated robots in each environmental configuration. $N = 6$ repetitions with nine intervals each. (**b**) Box & whisker diagram of those phases that used a dimmed light without any other competing light (phases 1 and 4) versus those phases that used a dimmed light that was competed by a bright light (phases 2 and 3). $N = 12$ per arena competition status with nine intervals each. The small sun-like symbols in the upper sections of the graphs represent the lights' intensities at the respective light. A striped sun indicates that the light was dimmed; a white sun indicates that the light was bright and the black sun indicates that the light was switched off

6. Питер Миллер, «Роевой интеллект», National Geographic, Россия, август 2007

Тезисы:

1. Животные действуют в интересах группы
2. Нет начальников и подчиненных
3. Каждая особь соблюдает набор простых правил
4. Один и тот же муравей может сегодня работать зодчим, а завтра мусорщиком. Как?
    a. Для того чтобы фуражир принял решение покинуть муравейник, ему необходимо встретиться с патрульным определенное количество раз, и промежуток между встречами не должен превышать десяти секунд
    b. Ученые пришли к выводу, что частота встреч с патрульными помогает фуражирам оценить безопасность обстановки за пределами гнезда (если встречи происходят с равными интервалами, значит, пора идти на поиски пищи; если нет — лучше подождать: возможно, снаружи слишком ветрено или рядом с муравейником притаилась голодная ящерица).
5. Как пчёлы ищут новое место для улья?
    a. Ученые расставили пять ульев, и только один из них обладал идеальными параметрами. Пчелы-разведчицы вскоре отыскали их все, и, вернувшись обратно к рою, каждая из них исполнила своеобразный танец, призывая своих коллег слетать и оценить то дупло, которое ей приглянулось. В этих движениях зашифрована информация о местонахождении и качестве новой жилплощади. Чем лучше найденная квартира, тем усерднее будет исполнен танец.
    b. Окончательное решение принимали разведчицы. Как только у входа в дупло собиралось около пятнадцати пчел, они решали, что кворум в наличии, и спешили обратно, чтобы обменяться новостями. Затем они подавали рою сигнал, что выбор сделан и пришла пора двигаться в путь. Как только все пчелы были готовы к полету, они отправлялись к своему новому жилищу, которым, конечно же, становился самый удобный из пяти ульев.
6. Как у игроков на скачках получается так точно предсказывать результаты заездов? Прогнозы скачек, появляющиеся на табло тотализатора перед стартом, почти всегда оказываются верными. Лошадь, на которую поставило большинство игроков, приходит первой, следующая по списку — второй и так далее. Причина в том, что тотализатор — это практически идеальный пример проявления интеллекта толпы.
7. У голубей нет вожака, который отдавал бы им приказы. Каждый из них, кружа в небе, пристально наблюдает за поведением своих ближайших соседей и следует нескольким простым правилам. Эти правила составляют основу другой формы роевого интеллекта, служащей не столько для принятия правильного решения, сколько для точной координации движений.
8. Подобные возможности заинтересовали Крейга Рейнолдса, специалиста в области компьютерной графики. В 1986 году он создал простую на первый взгляд программу, в которой участвовали похожие на птиц роботы, или «птицоиды». Они должны были соблюдать следующие три правила: во-первых, не сталкиваться со своими собратьями, во-вторых, выбирать среднюю траекторию полета, ориентируясь на соседей, и, в-третьих, держаться поблизости от остальных роботов. Когда модель начали тестировать, на экране компьютера очень достоверно был воспроизведен полет птичьей стаи и даже ее хаотичные метания (точь-в-точь как в реальности).

9. Это поведение довольно часто применяется в групповой робототехнике.
10. Рыбы по поведению соседей сразу же чувствуют, что что-то не так, поэтому известие о приближении врага в мгновение ока облетает весь косяк
11. Говорим ли мы о муравьях, пчелах, голубях или о карибу, налицо неизменные принципы «умного» группового поведения: отсутствие «центра управления», умение оценивать обстановку, соблюдение простых правил. Именно так рождается эффективная стратегия, позволяющая этим существам с успехом выходить из сложных ситуаций. В этом и заключается притягательная сила роевого интеллекта.
12. Толпа может быть умной, только если индивиды несут ответственность за свои действия и самостоятельно принимают решения. Если же они будут слепо копировать поведение друг друга, удовлетворять только свои прихоти или ждать, что кто-то подскажет им, что делать, коллектив не сможет функционировать успешно.

7. Cooperation through self-assembly in multi-robot systems

Tuci E., GroЯ R., Trianni V., Mondada F., Bonani M., Dorigo M.

ACM TAAS, Volume 1(2), 115-150, December 2006

Abstract

This paper illustrates the methods and results of two sets of experiments in which a group of mobile robots, called *s-bots*, are required to physically connect to each other—i.e., to self-assemble—to cope with environmental conditions that prevent them to carry out their task individually. The first set of experiments is a pioneering study on the utility of self-assembling robots to address relatively complex scenarios, such as cooperative object trasport. The results of our work suggest that the *s-bots* possess hardware characteristics which facilitate the design of control mechanisms for autonomous self-assembly. The second set of experiments is an attempt to integrate within the behavioural repertoire of an *s-bot* decision making mechanisms to allow the robot to autonomously decide whether or not environmental contingencies require self-assembly. The results show that it is possible to synthesise, by using evolutionary computation techniques, artificial neural networks that integrate both the mechanisms for sensory-motor coordination and for decision making required by the robots in the context of self-assembly.

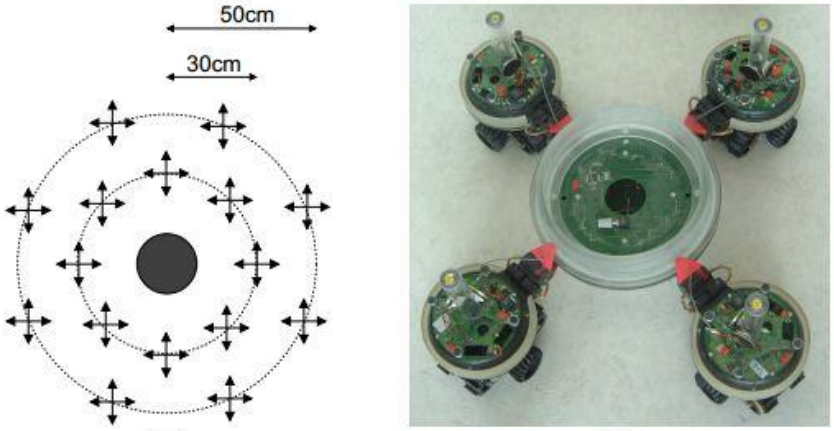

Figure 6: (a) Potential starting points and orientations of the *s-bots* around the *prey*. (b) Four *s-bots* connected in "star-like" formation around the prey.

Algorithm I - The assembly module

```
1  activate colour ring in blue
2  repeat
3     (N1, N2) ← featureExtraction(camera)
4     (N3, N4) ← sensorReadings(proximity)
5     (N5, N6, N7) ← neuralNetwork(N1, N2, N3, N4)
6
7     if (N7 > 0.5) ∧ (grasping requirements fulfilled)
8        then
9              grasp
10             if (successfully connected)
11               then
12                    activate colour ring in red
13                    activate transport module
14               else
15                    open gripper
16             fi
17    fi
18    apply (N5, N6) to tracks
19 until timeout reached
```

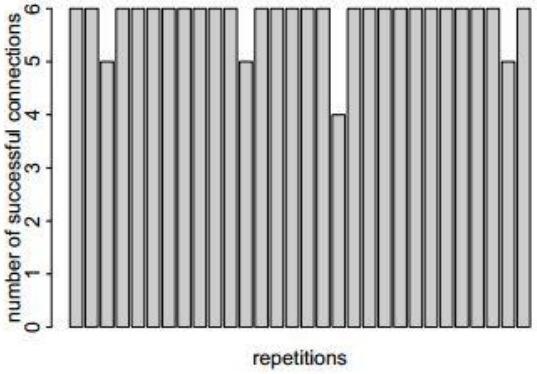

(a)

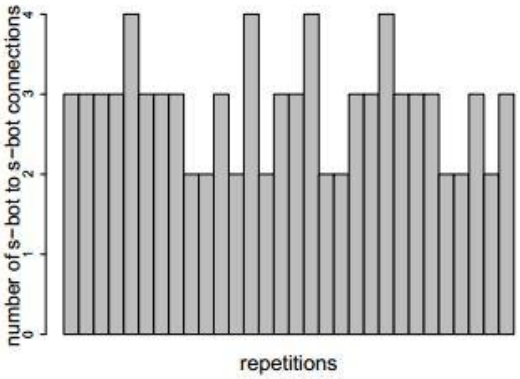

(b)

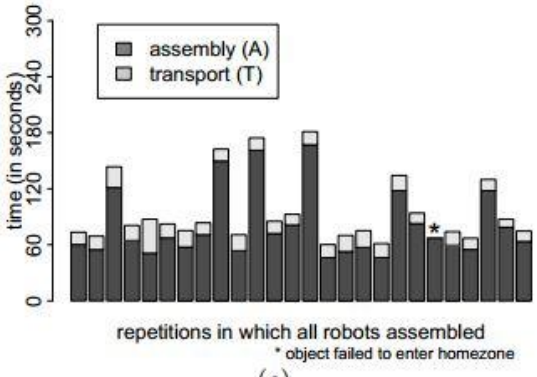

(c)

Figure 9: (a) Number of robots successfully connected. (b) Number of *s-bot* to *s-bot* connections. (c) Time period the group was busy self-assembling and transporting the *prey* inside the target zone.

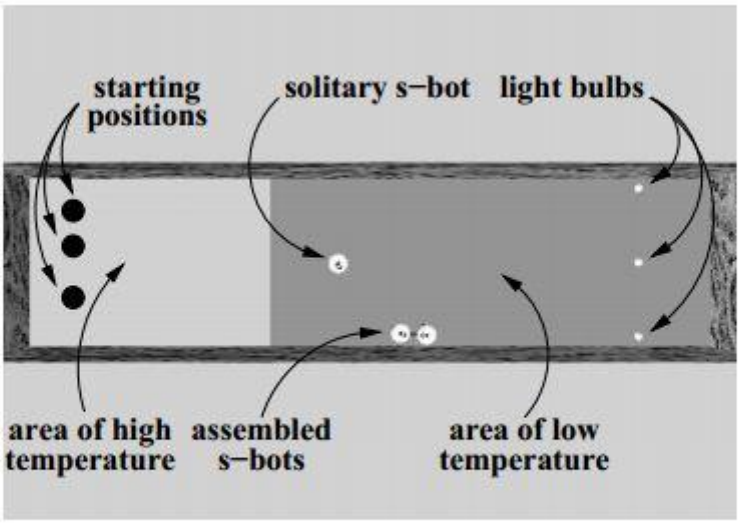

Figure 10: A graphical representation of the task. See text for details.

8. IR-based Communication and Perception in Microrobotic Swarms S. Kornienko, S. Kornienko Institute of Parallel and Distributed Systems, University of Stuttgart, Universit□atsstr. 38, D-70569 Stuttgart, Germany

Abstract

In this work we consider development of IR-based communication and perception mechanisms for real microrobotic systems. It is demonstrated that a specific combination of hardware and software elements provides capabilities for navigation, objects recognition, directional and unidirectional communication. We discuss open issues and their resolution based on the experiments in the swarm of microrobots "Jasmine".

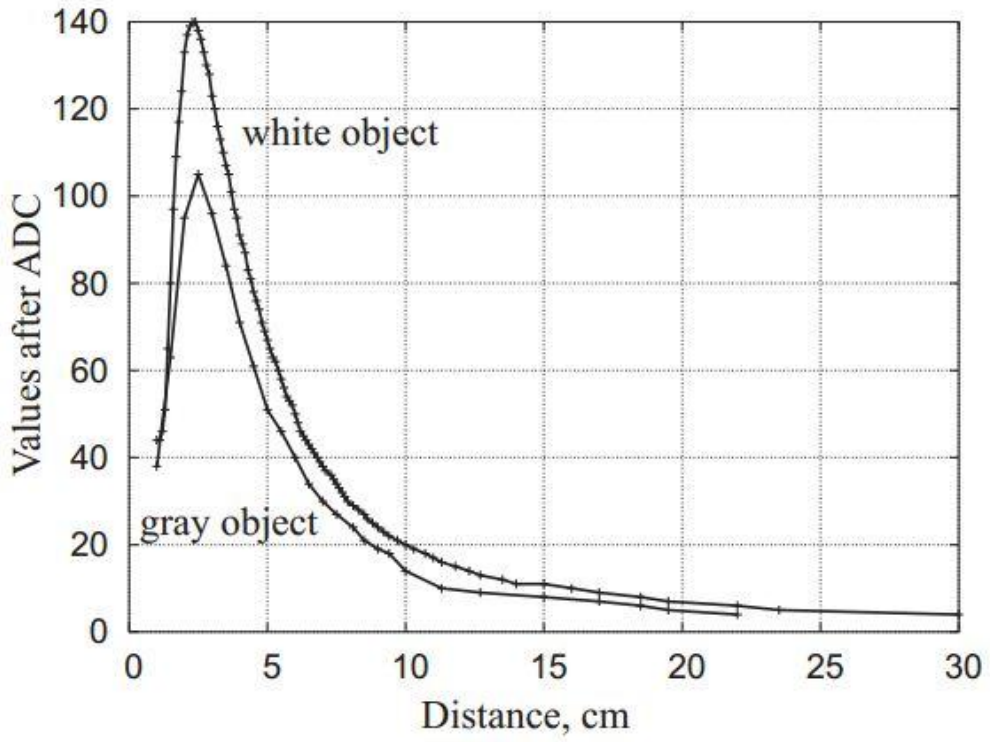

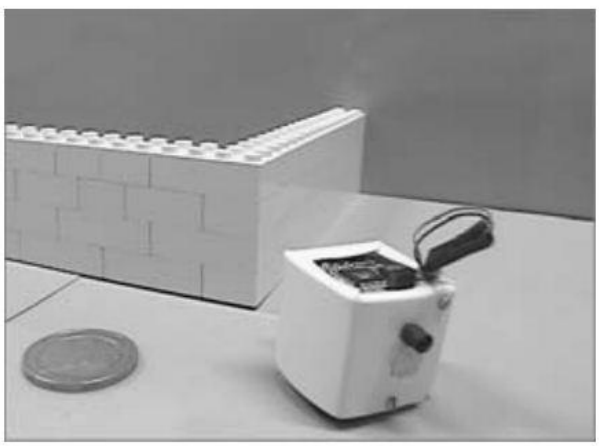

(a)

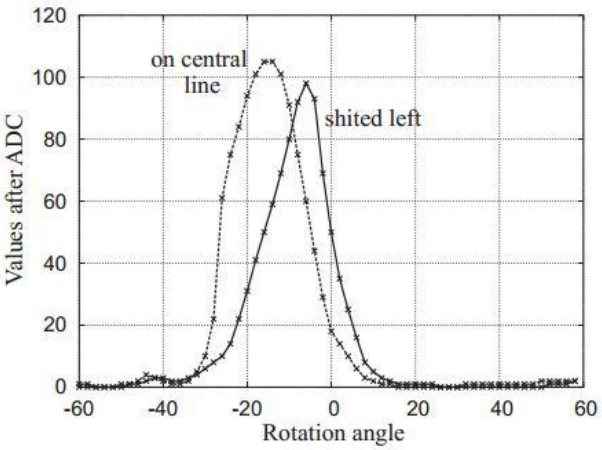

(b)

9. Cooperative Hole Avoidance in a *Swarm-bot*

Trianni V., Nolfi S., Dorigo M.

***Robotics and Autonomous Systems*, Volume 54, number 2, pp. 97-103**

Abstract

In this paper, we study coordinated motion in a swarm robotic system, called a *swarm-bot*. A *swarm-bot* is a self-assembling and self-organising artifact, composed of a swarm of *s-bots*, mobile robots with the ability to connect to and disconnect from each other. The *swarm-bot* concept is particularly suited for tasks that require all-terrain navigation abilities, such as space exploration or rescue in collapsed buildings. As a first step toward the development of more complex control strategies, we investigate the case in which a *swarm-bot* has to explore an arena while avoiding falling into holes. In such a scenario, individual *s-bots* have sensory-motor limitations that prevent them navigating efficiently. These limitations can be overcome if the *s-bots* are made to cooperate. In particular, we exploit the *s-bots*' ability to physically connect to each another. In order to synthesise the *s-bots*' controller, we rely on artificial evolution, which we show to be a powerful tool for the production of simple and effective solutions to the hole avoidance task.

Keywords: evolutionary robotics, swarm intelligence, swarm robotics, swarm-bot

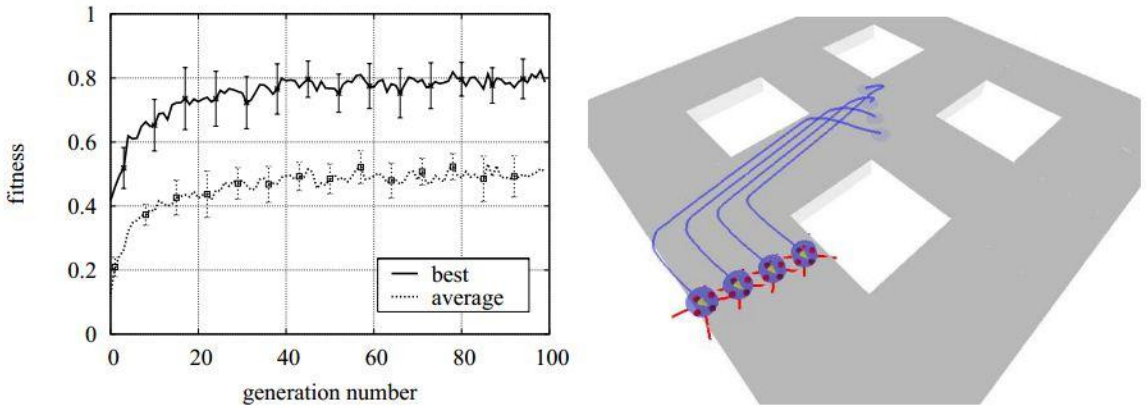

Figure 2: Hole avoidance results: (a) Average fitness over 10 replications of the experiment. (b) Trajectories displayed by a *swarm-bot* performing hole avoidance.

Table 1: Performance of the best individuals for each replication of the experiment, averaged over 100 trials. The mean value and the standard deviation are reported.

Replication	1	2	3	4	5	6	7	8	9	10
Fitness Avg.	0.66	0.65	0.65	0.61	0.58	0.64	0.69	0.64	0.66	0.65
Fitness Std.	0.14	0.12	0.14	0.19	0.10	0.16	0.12	0.15	0.13	0.16

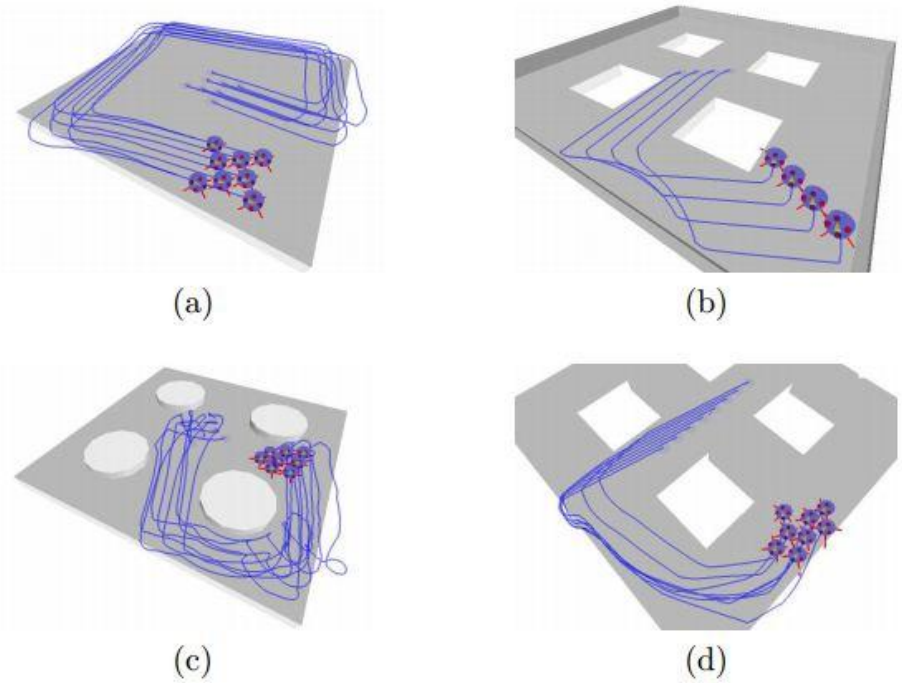

Figure 3: Generalisation properties. The trajectories and the final position of the *swarm-bot* are shown. (a) Size and shape change. A "star" formation is tested in a square arena (grey area) without holes but with open borders. The trajectories indicates that the *swarm-bot* is able to avoid falling out, even if some *s-bots* are pushed out from the border. (b) Obstacle avoidance. The square arena with holes (grey area) is surrounded by walls (dark grey borders). The *swarm-bot* proves able to avoid both holes and obstacles. (c) Obstacle and hole avoidance of a "star" formation with flexible connections. Here the cylindrical obstacles (light grey objects) create a narrow passage with the edge of the arena (grey area), which is faced by the *swarm-bot* trough reconfiguration of its shape. (d) Hole avoidance of a big linear formation with flexible connections. Here the *swarm-bot* completely deforms when it reaches the edge of the arena (grey area), therefore adapting its shape.

10. Dimos V. Dimarogonas, Kostas J. Kyriakopoulos; Connectedness Preserving Distributed Swarm Aggregation for Multiple Kinematic Robots. In IEEE TRANSACTIONS ON ROBOTICS, VOL. 24, NO. 5, OCTOBER 2008

***Abstract*—A distributed swarm aggregation algorithm is developed for a team of multiple kinematic agents. Specifically, each agent is assigned a control law, which is the sum of two elements: a repulsive potential field, which is responsible for the collision avoidance objective, and an attractive potential field, which forces the agents to converge to a configuration where they are close to each other. Furthermore, the attractive potential field forces the agents that are initially located within the sensing radius of an agent to remain within this area for all time. In this way, the connectivity properties of the initially formed communication graph are rendered invariant for the trajectories of the closed-loop system. It is shown that under the proposed control law, agents converge to a configuration where each agent is located at a bounded distance from each of its neighbors. The results are also extended to the case of nonholonomic kinematic unicycle-type agents and to the case of dynamic edge addition. In the latter case, we derive a smaller bound in the swarm size than in the static case.**

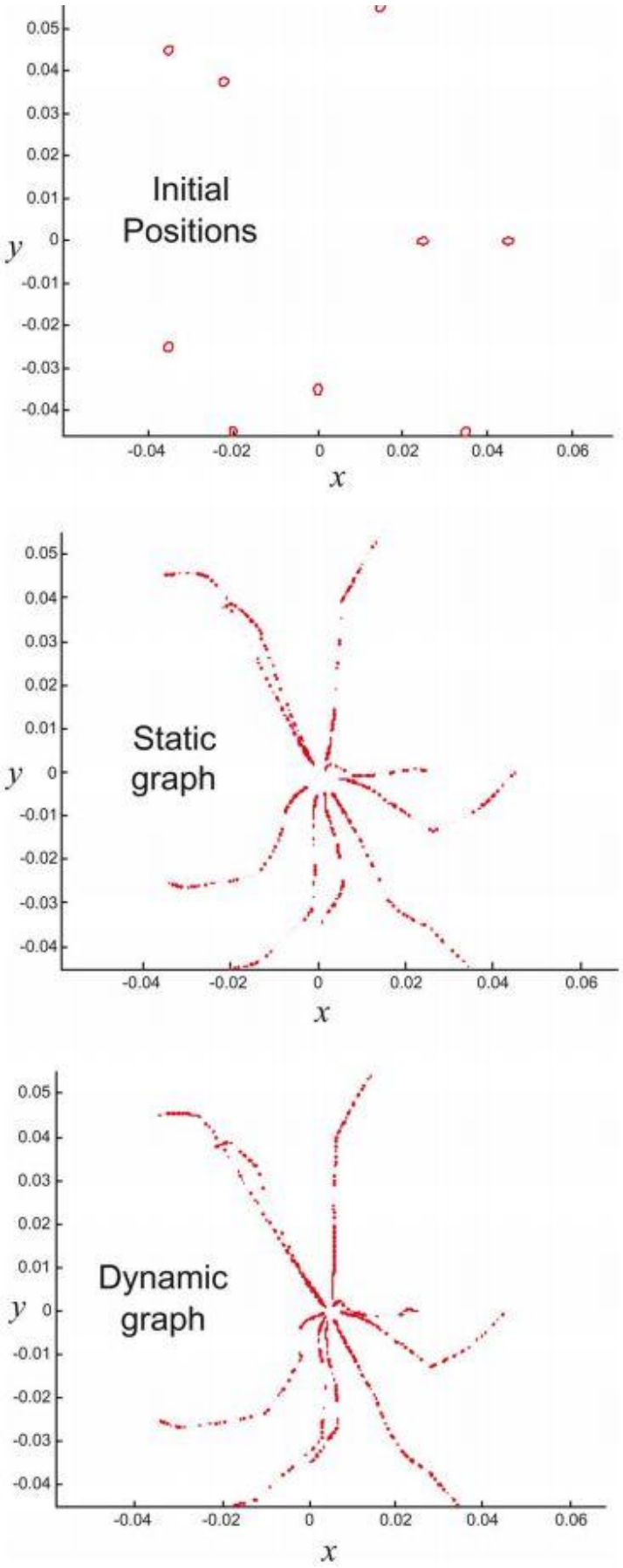

Fig. 2. Evolution in time of the swarm under (middle) control law (4) for the static communication graph case and (bottom) control law (12) for the dynamic graph case. The communication graph is connected in both cases. The second control law leads to a smaller swarm size.

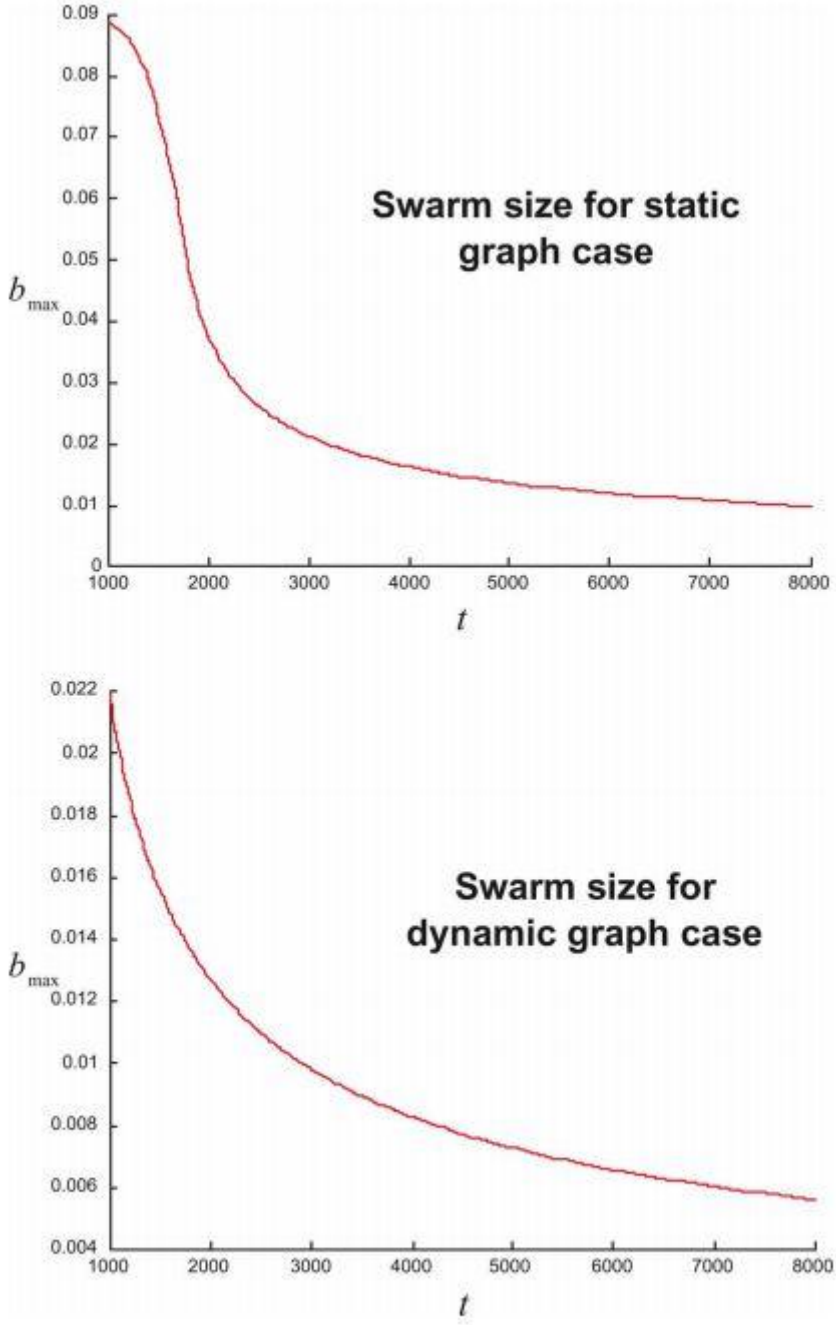

Fig. 3. Evolution of the swarm size for the two simulations of Fig. 2. The dynamic graph formulation leads to a smaller swarm size.

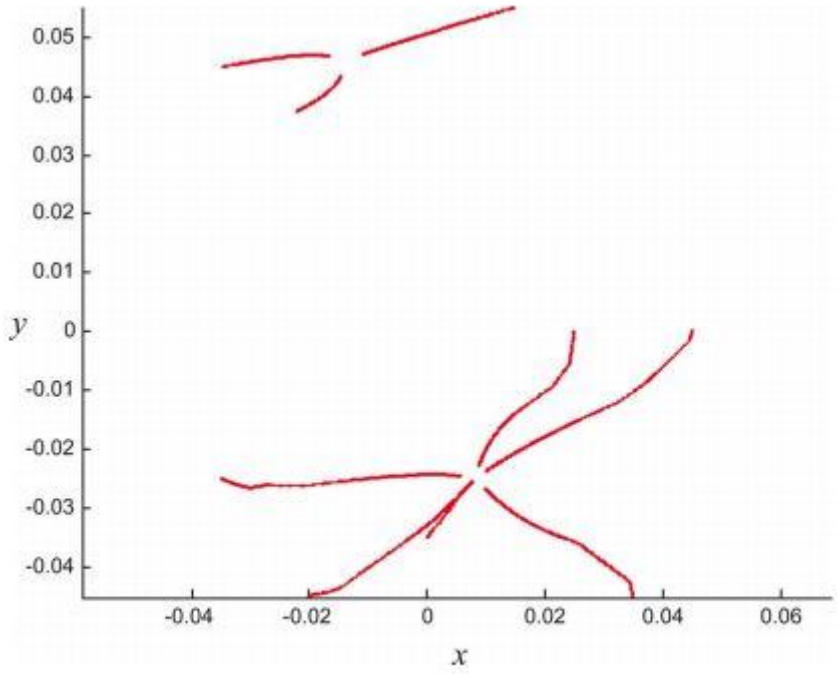

Fig. 4. Lack of connectivity in the initially formed communication graph decouples the swarm into its connected components.

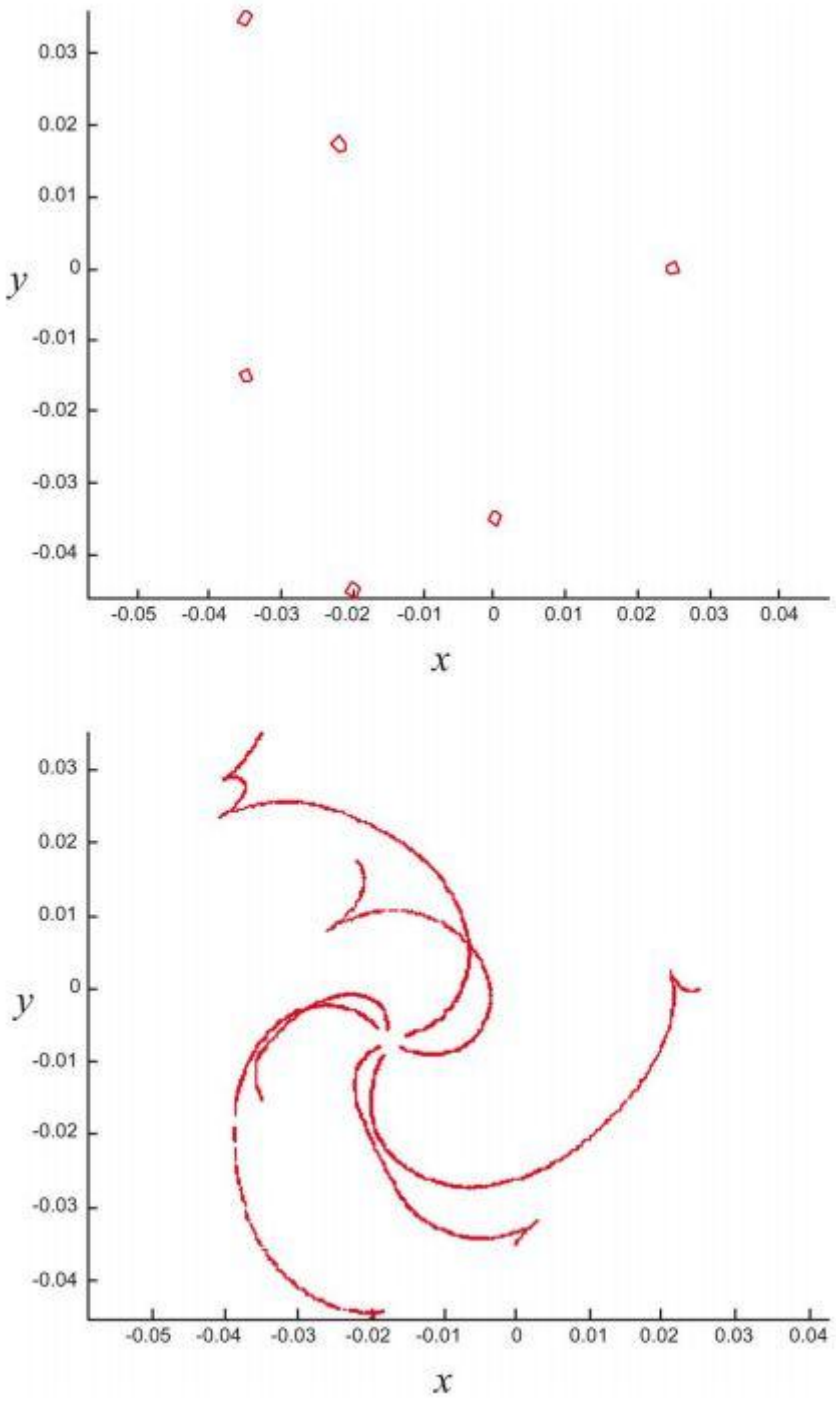

Fig. 5. Evolution in time of the nonholonomic swarm under control laws (9) and (10). The communication graph is connected.

11. Schmickl, Thomas; Crailsheim, Karl: Trophallaxis within a robotic swarm: Bio-inspired communication amongrobots in a swarm, in: Autonomous Robots 25 (1-2) (2008), 171 - 188.

Abstract This article presents a bio-inspired communication strategy for large-scale robotic swarms. The strategy is based purely on robot-to-robot interactions without any central unit of communication. Thus, the emerging swarm regulates itself in a purely self-organized way. The strategy is biologically inspired by the trophallactic behavior (mouth-to-mouth feedings) performed by social insects. We show how this strategy can be used in a collective foraging scenario and how the efficiency of this strategy can be shaped by evolutionary computation. Although the algorithm works stable enough that it can be easily parameterized by hand, we found that artificial evolution could further increase the efficiency of the swarm's behavior. We investigated the suggested communication strategy by simulation of robotic swarms in several arena scenarios and studied the properties of some of the emergent collective decisions made by the robots. We found that our control algorithm led to a nonlinear, but graduated path selection of the emerging trail of loaded robots. They favored the shortest path, but not all robots converged to this trail, except in arena setups with extreme differences in the length of the two possible paths. Finally, we demonstrate how the flexibility of collective decisions that arise through this new strategy can be used in changing environments. We furthermore show the importance of a negative feedback in an environment with changing foraging targets. Such feedback loops allow outdated information to decay over time. We found that task efficiency is constrained by a lower and an upper boundary concerning the strength of this negative feedback.

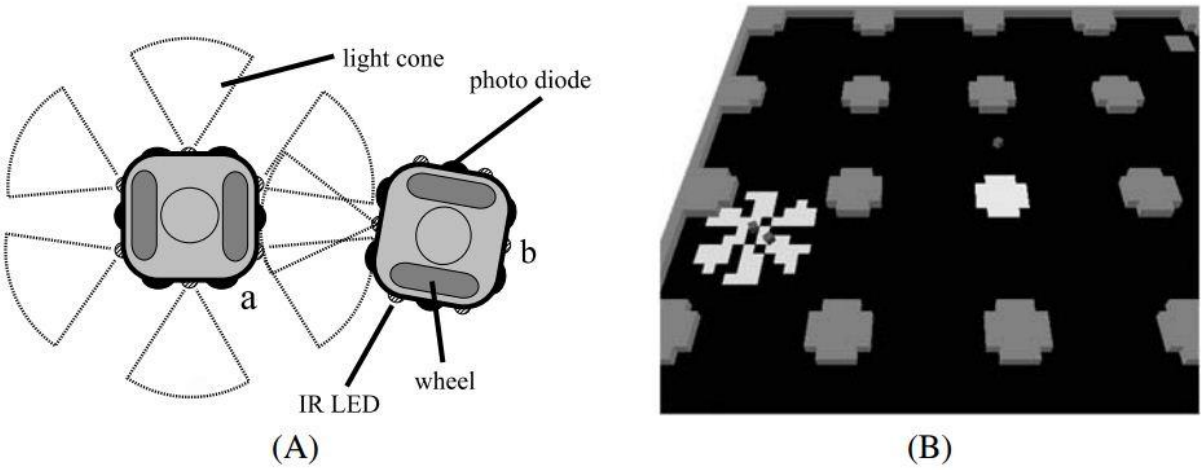

Fig. 1 **A** Morphology of the robots in the used simulation environment with special emphasis on the communication systems (infrared LEDs, photo-diodes) and on the movement systems. In this picture, the two robots can establish a bi-directional communication. All 6 light cones of robot "a" are drawn; only the one light cone that is involved into a communication channel is drawn for robot "b". **B** Equivalent picture of the communication-light-beams in our simulator. The focal robot can

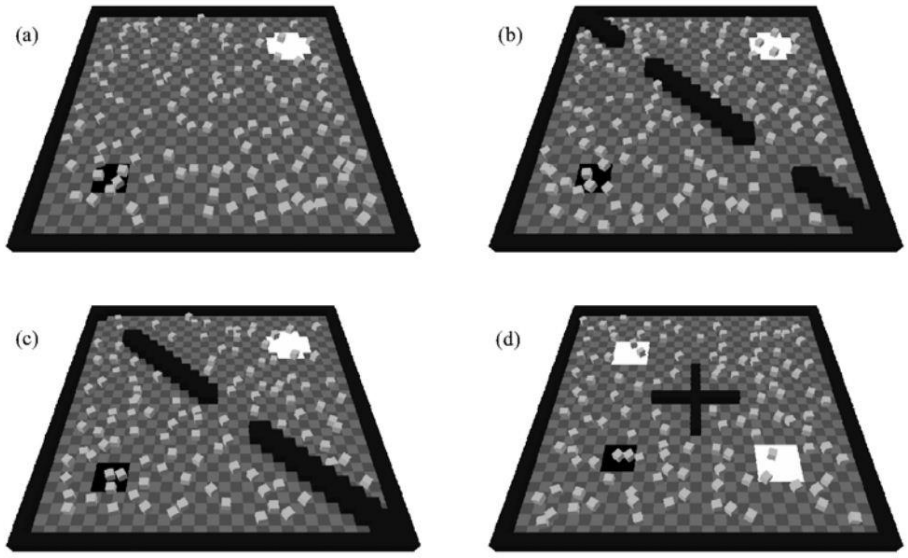

Fig. 2 Screenshots of all environments in which we tested our swarms. The black ground patches indicate dirt areas in all pictures; the white spot indicated the dump area. The little gray boxes represent the robots in our simulation platform. **a** The most simple environment. Robots could directly pass from the dirt area to the dump area. **b** The robots could move through two equidistant gates to pass from the dirt area to the dump area. **c** The same setup, but now one gate offers a shorter path. **d** The setup with a changing environment: At first, only the dump in the upper left corner is available. After the robots dropped almost all dirt particles there, the dump area is shifted to the lower right corner. The robots have to pick up the dirt particles again and to move them over to the new dump position

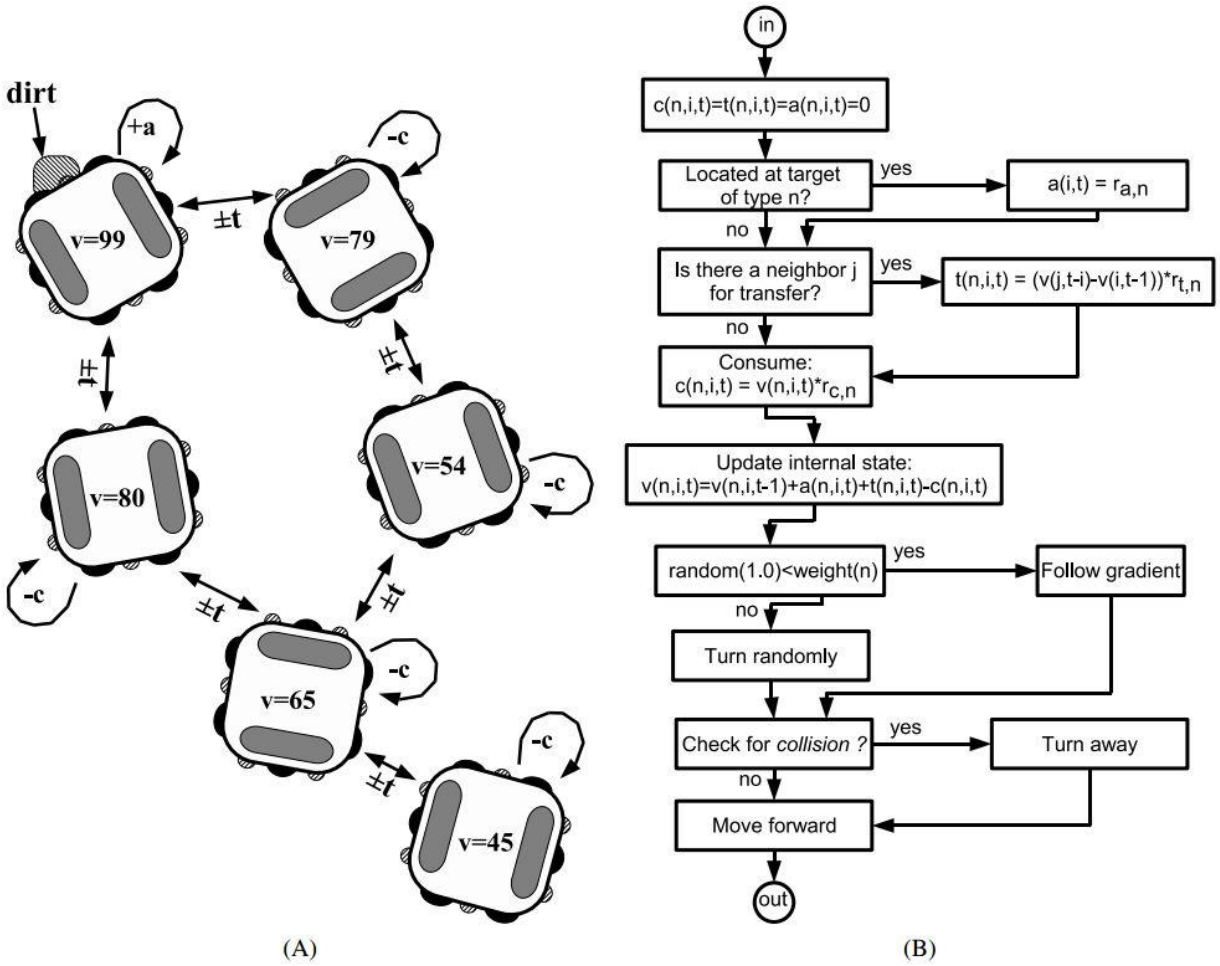

Fig. 3 **A** This scheme shows the basic principles of the "trophallaxis derived control strategy". Robot 1 finds a piece of dirt and increases its internal variable v by the given addition rate (indicated as "$+a$"). All robots constantly decrease their internal variable v by the given consumption rate (indicated as "$-c$"). The variable v is constrained to be above zero. All robots that are near enough to establish a robot-to-robot communication link communicate their current values of v and transfer a fraction of the encountered difference from the robot with the higher value of v to the robot with the lower value of v(as it is

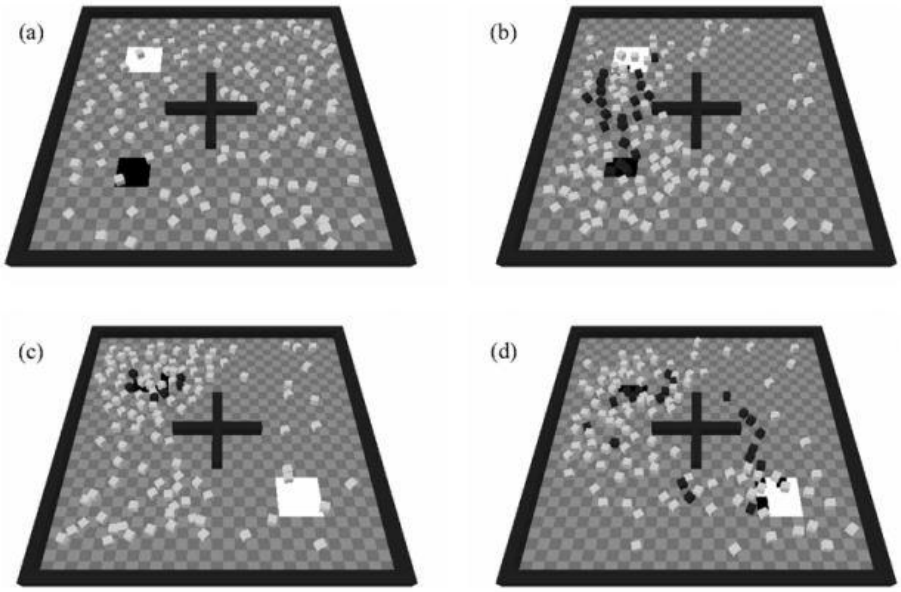

Fig. 11 Screenshots of the robotic swarm that performs its cleaning task in a changing environment. Black floor patches: dirt particles, white floor patches: dump area, grey boxes: empty robots, dark boxes; loaded robots. **a** Initial settings. **b** The loaded robots directly approach the dump area uphill the gradient of v_2. **c** The dump is shifted to the lower right corner of the arena; only a few empty robots occupy this area. **d** The robots pick up the dirt items again and approach the new dump area on two trails around the obstacle (cross-shaped wall) in the center of the arena

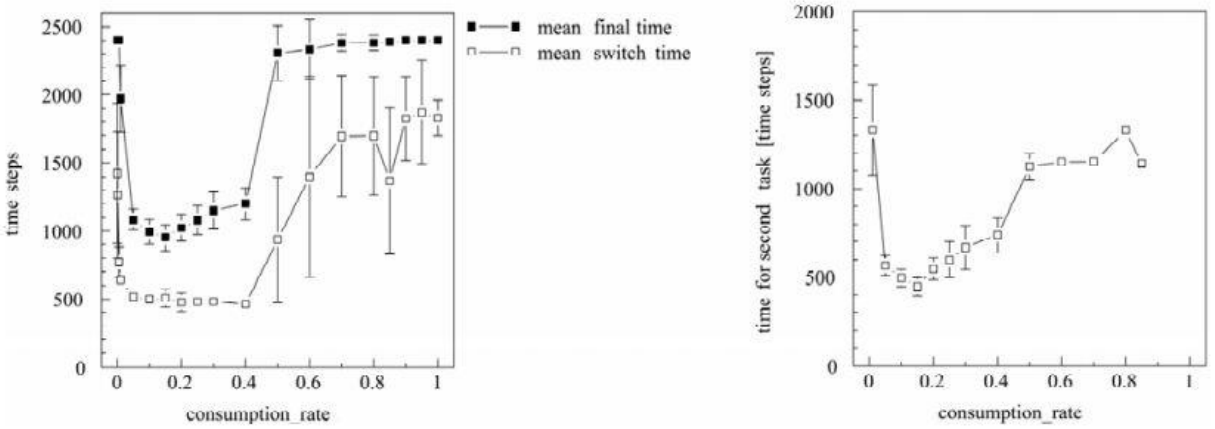

Fig. 12 Efficiency of work performed in the changing environment and with varying values of the consumption-rate ($r_{c,2}$). **a** With very low values of the parameter $r_{c,2}$, the swarm of robots needed very long to finish even the first part of the task (prior to the environmental fluctuation). This can be seen by the high values of the "mean switch time". Higher values of $r_{c,2}(\geq 0.05)$ lead to quick delivery of particles at the first dump site and also to a quick movement of these particles to the shifted dump area ("mean final time"). Very high values of $r_{c,2}(\geq 0.7)$ lead again to a low performance of the swarm in the fluctuating environment. **b** With low values ($r_{c,2} < 0.05$) and with high values ($r_{c,2} > 0.4$) of the parameter $r_{c,2}$, also the time-span between the triggering of the environmental fluctuation and the final success time is maximized. In this figure only those runs were considered that succeeded to finish the second task before the end of the runtime of the experiment (2400 time steps). $N = 10$ per setting

12. Schmickl, Thomas; Moeslinger, Christoph; Crailsheim, Karl: Collective perception in a robot swarm., in: Lecture Notes in Computer Science 4433 (2007), 144 - 157.

Abstract. In swarm robotics, hundreds or thousands of robots have to reach a common goal autonomously. Usually, the robots are small and their abilities are very limited. The autonomy of the robots requires that the robots' behaviors are purely based on their local perceptions, which are usually rather limited. If the robot swarm is able to join multiple instances of individual perceptions to one big global picture (e.g. to collectively construct a sort of map), then the swarm can perform efficiently and such a swarm can target complex tasks. We here present two approaches to realize 'collective perception' in a robot swarm. Both require only limited abilities in communication and in calculation. We compare these strategies in different environments and evaluate the swarm's performance in simulations of fluctuating environmental conditions and with varying parameter settings.

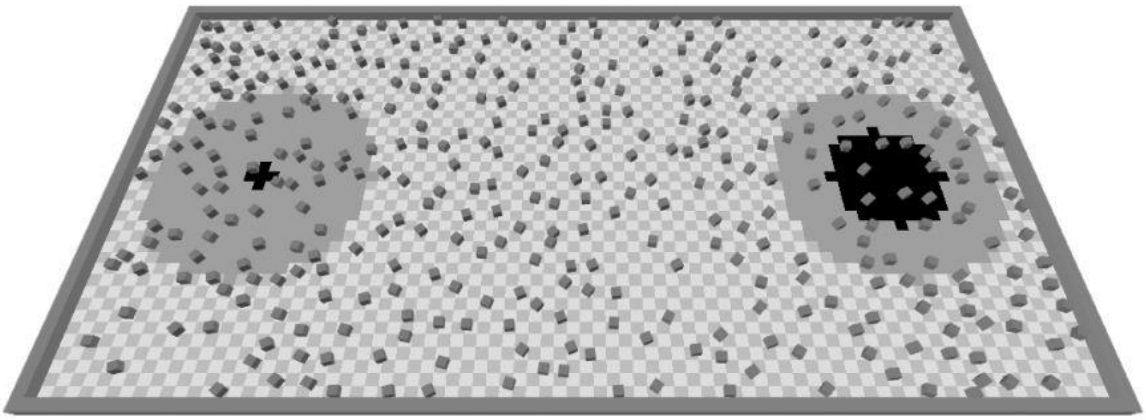

Fig. 1. A screen shot of our simulation platform LaRoSim. The two black areas (small left and huge right) represent target areas for aggregation. The gray circles indicate the zones in which we counted the robots for evaluating the aggregation success. Gray boxes represent robots.

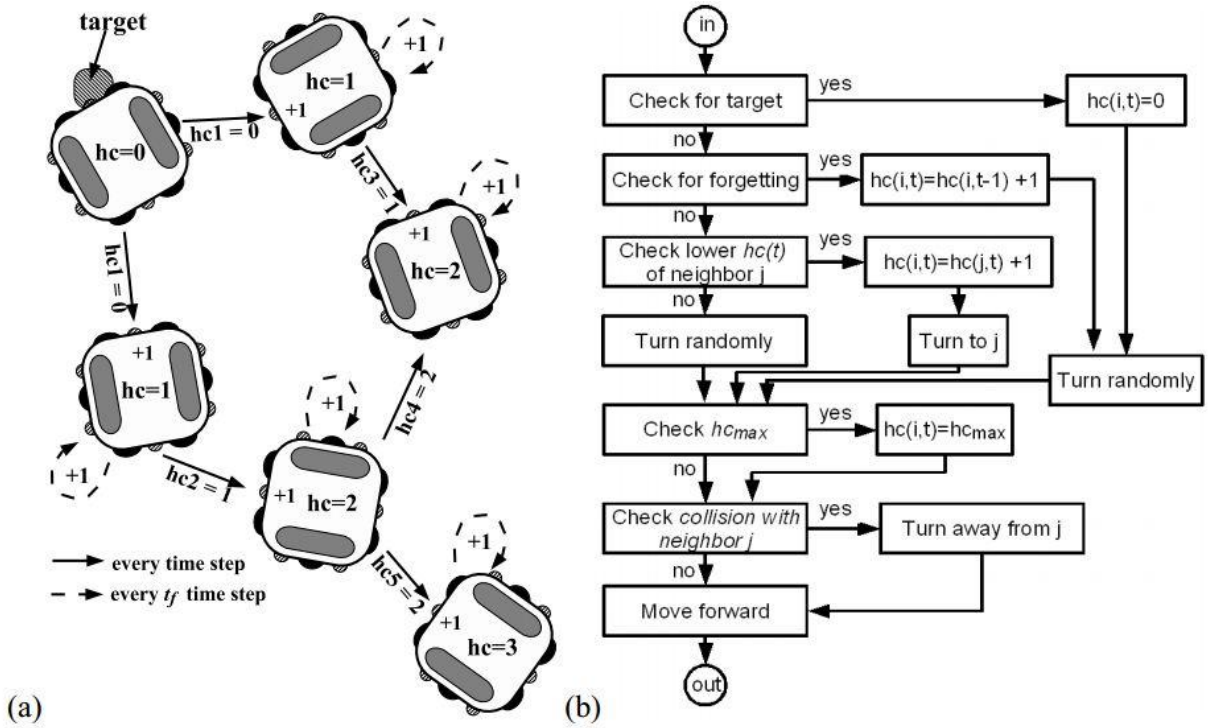

Fig. 3. (a) The gradient of hop-counts that emerges in the 'hop-count' strategy. The robot on the target sets its hop-count to 0. All robots copy the lowest hop-count from their neighbors and increase it by 1. After some ($\mathbf{t_f}$) time steps, they increase the hop-count spontaneously ('forgetting'). (b) Behavioral program of a robot in the 'hop-count' strategy. This program is executed every time step.

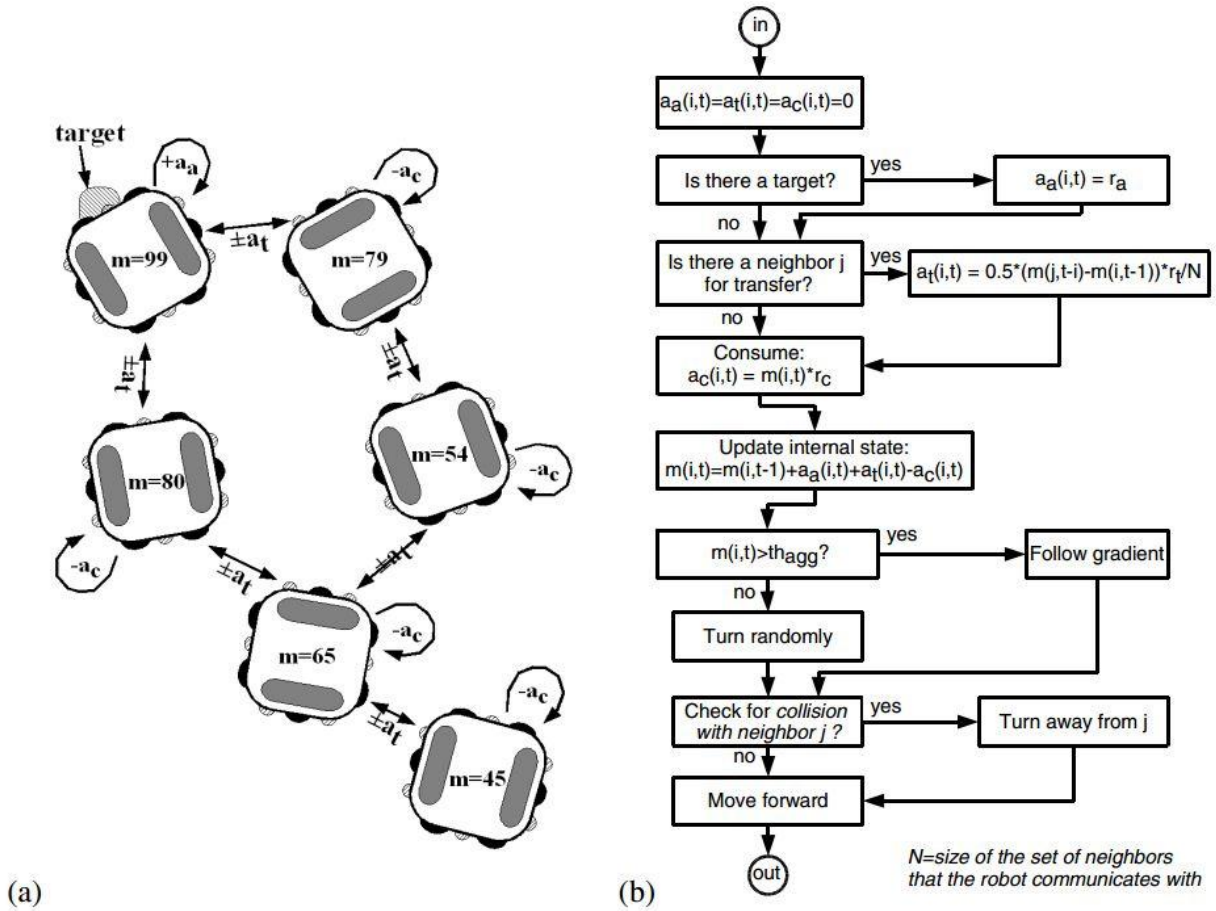

Fig. 4. (a) The gradient of 'virtual nectar' that emerges in the 'trophallaxis-inspired' strategy. The robot at the target adds 'virtual nectar' to its memory. All robots exchange fractions of the 'virtual nectar' proportionally to the inter-robot differences. All robots consume 'virtual nectar' over time, thus they decrease their memory values ('forgetting'). (b) Behavioral program of a robot in the 'trophallaxis-inspired' strategy. This program is executed every time step.

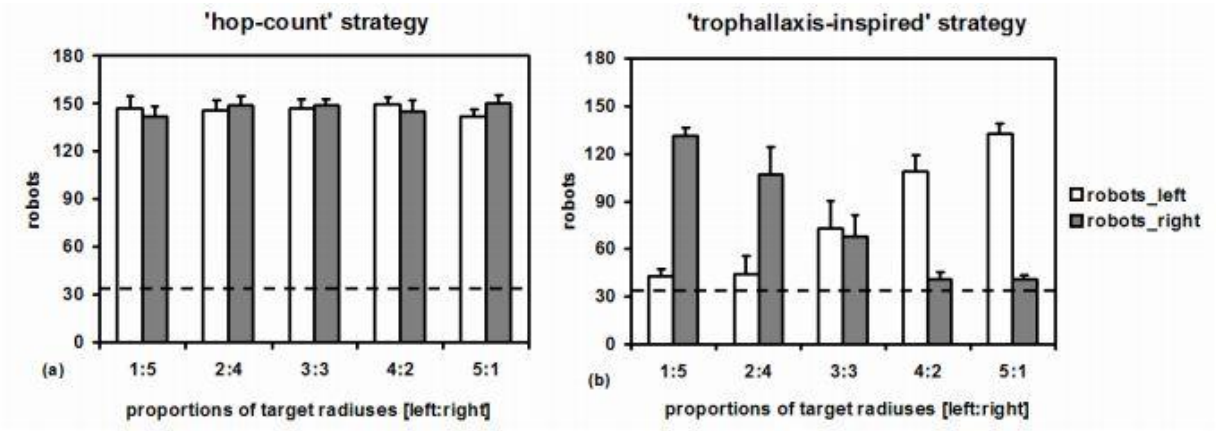

Fig. 5. Collective decisions made by the robot swarm in different environments. The dashed line shows the expected number of robots that would have been in the measurement area (radius=10 each) if there had been no aggregation behavior at all. N=10 per setting. Bars represent mean values and whiskers indicate standard deviations. Duration: 250 time steps.

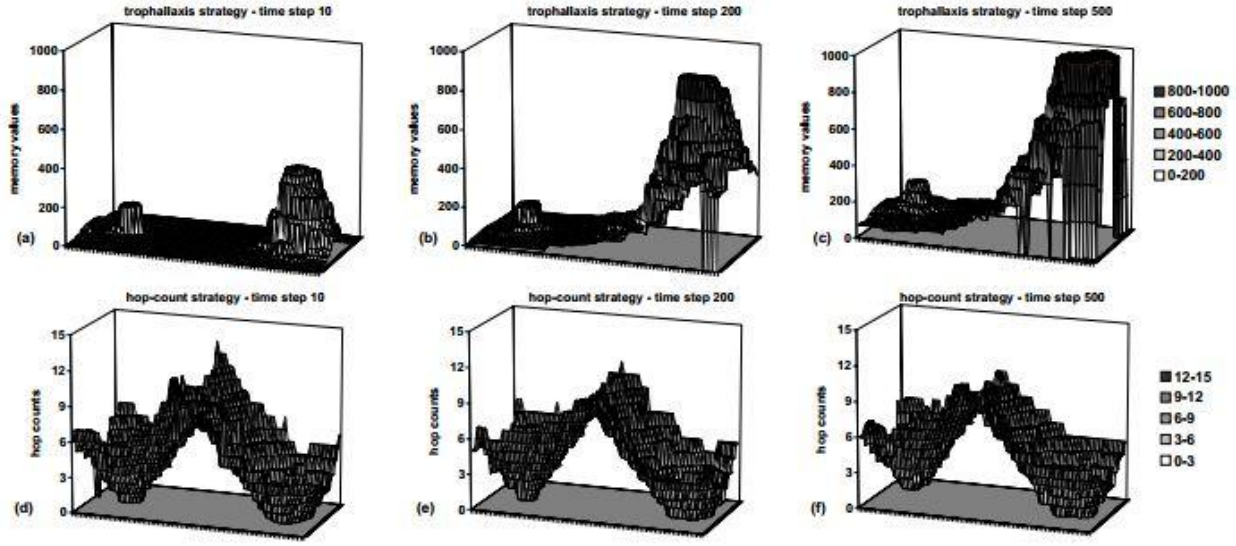

Fig. 6. The dynamics of the emerging gradients in our experiment. (a-c): The dynamics of the gradient in the trophallaxis inspired strategy. For generating the picture, we assigned the maximum memory value of all visible robots to each location in the arena. (d-f): The dynamics of the gradient in the hop-count strategy. Here we assigned the minimum hop-count of all visible robots to each position in the arena. Both simulation runs used extreme environmental conditions: The left target was very small (radius=1) and the right target was large (radius=5).

13. Schmickl, Thomas; Moeslinger, Christoph; Thenius, Ronald; Crailsheim, Karl: Individual adaptation allows collective path-finding in a robotic swarm, in: International Journal of Factory Automation, Robotics and Soft Computing (2007). (not published)

Abstract: **The coordination of an autonomous robotic swarm requires a control algorithm that is simple, scalable, robust and flexible. Biological systems show many kinds of behaviours, which enable organisms to act efficiently in a dynamic environment. By mimicking the trophallactic behaviour of honeybees (mouth-to-mouth feeding), we developed a communication scheme and a navigation algorithm for mobile robots. This allows a swarm of robots to perform collective decision-making based on individual robot navigation. In this article we present a novel feature of this algorithm: It allows a robotic swarm to react to the shape and to the orientation of areas of unsuitable terrain. We demonstrate that a robotic swarm using this new algorithm is able to make near-optimal route choices, i.e. whether to cross or to avoid an area with unsuitable terrain.**

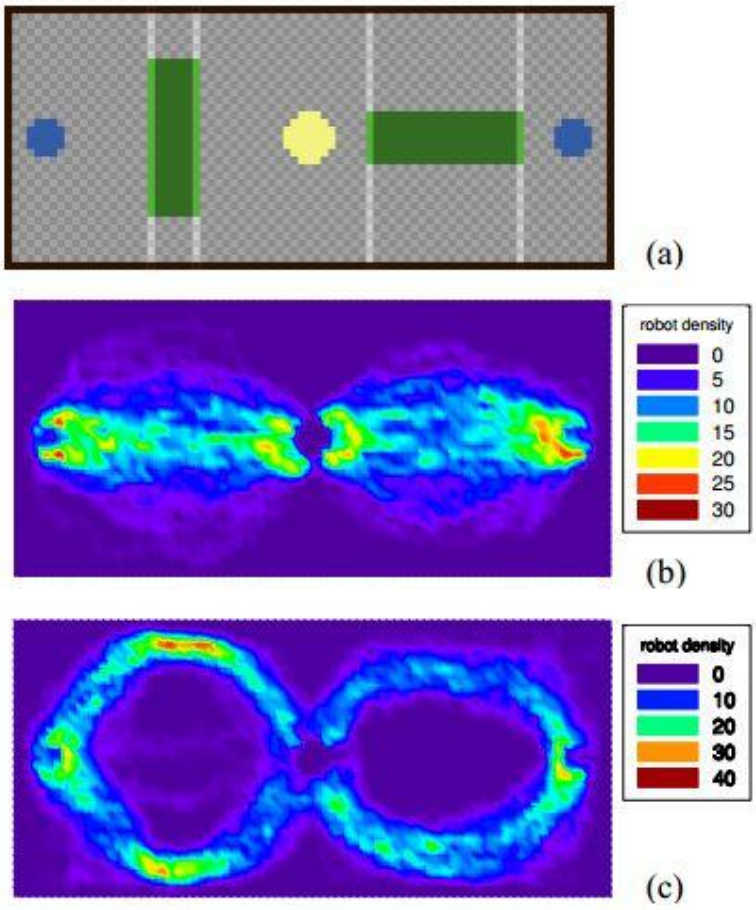

Fig1: (a) The arena setup with one dump (yellow) in the middle and two dust areas (blue) on the left side and on the right side. Two areas of unfavourable terrain (green) were placed in between. The four bright lines indicate the regions where we measured whether the robots moved on or off the unfavourable terrains. (b) The path densities of loaded robots when the value of κ (see equation 1.1) was set to 0. (c) The path densities of loaded robots when κ was set to 1000.

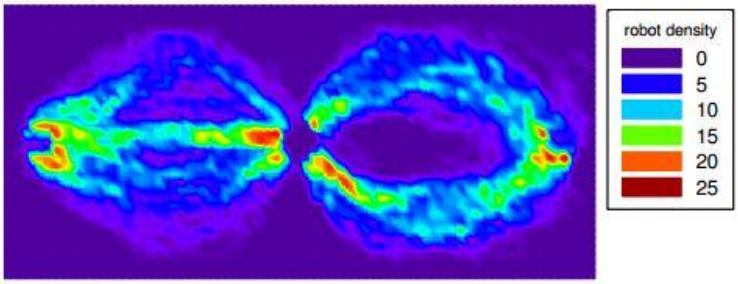

Fig3: Path densities of the loaded robots, moving from the outer dust areas towards the dump in the middle. Robots used the optimized values for r_c^{min} and κ.

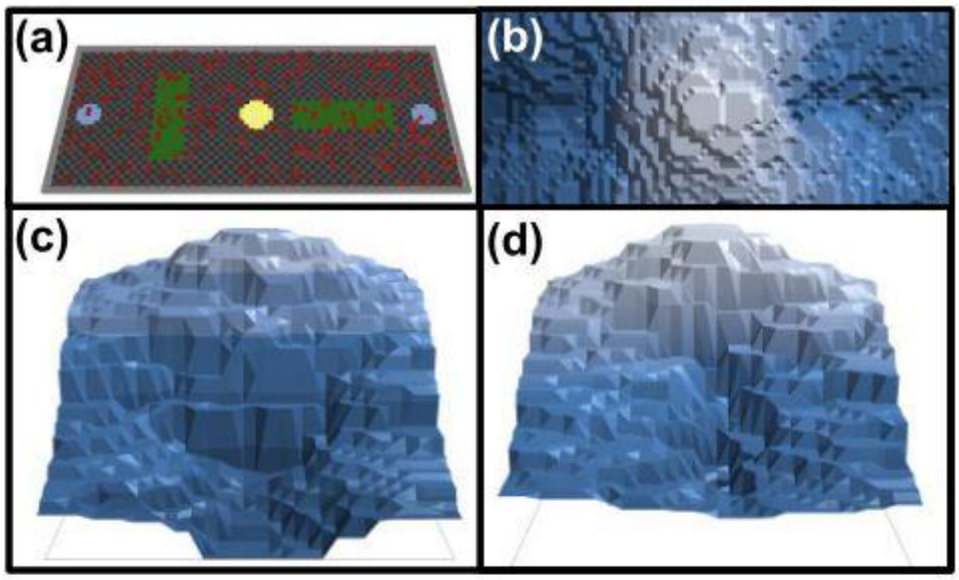

Fig4: Topology of the emerging gradient from the dump. For better representation the gradient was linearised using the function $\Omega(x,t)$ (see equation 4.1). (a) Arena setup. (b) View from above. (c) View from left. (d) View from right.

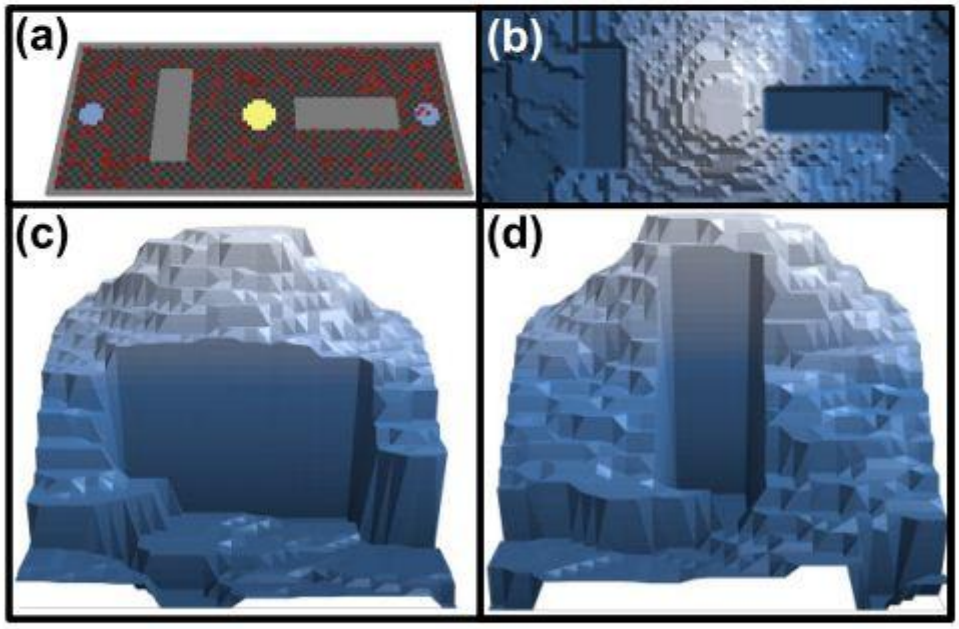

Fig5: Emerging gradients with solid walls (grey and rectangular objects) replacing the unfavourable terrains. For better representation the gradient was linearised using the function $\Omega(x,t)$ (see equation 4.1).(a) Arena setup. (b) View from above. (c) View from left. (d) View from right.

14. M. Hartbauer and H. Roemer; "A novel distributed swarm control strategy based on coupled signal oscillators". In Bioinspiration & Biomimetics, 2, 42-56 (2007)

Abstract

The miniaturization of microrobots is accompanied by limitations of signaling, sensing and agility. Control of a swarm of simple microrobots has to cope with such constraints in a way which still guarantees the accomplishment of a task. A recently proposed communication method, which is based on the coupling of signal oscillators of individual agents [13], may provide a basis for a distributed control of a simulated swarm of simple microrobots (similar to I-Swarm microrobots) engaged in a cleaning scenario. This self-organized communication method was biologically inspired from males of chorusing insects which are known for the rapid synchronization of their acoustic signals in a chorus. Signal oscillator properties were used to generate waves of synchronized signaling (s-waves) among a swarm of agents. In a simulation of a cleaning scenario, agents on the dump initiated concentrically spreading s-waves by shortening their intrinsic signal period. Dirt-carrying agents localized the dump by heading against the wave front. After optimization of certain control parameters the properties of this distributed control strategy were investigated in different variants of a cleaning scenario. These include a second dump, obstacles, different agent densities, agent drop-out and a second signal oscillator.

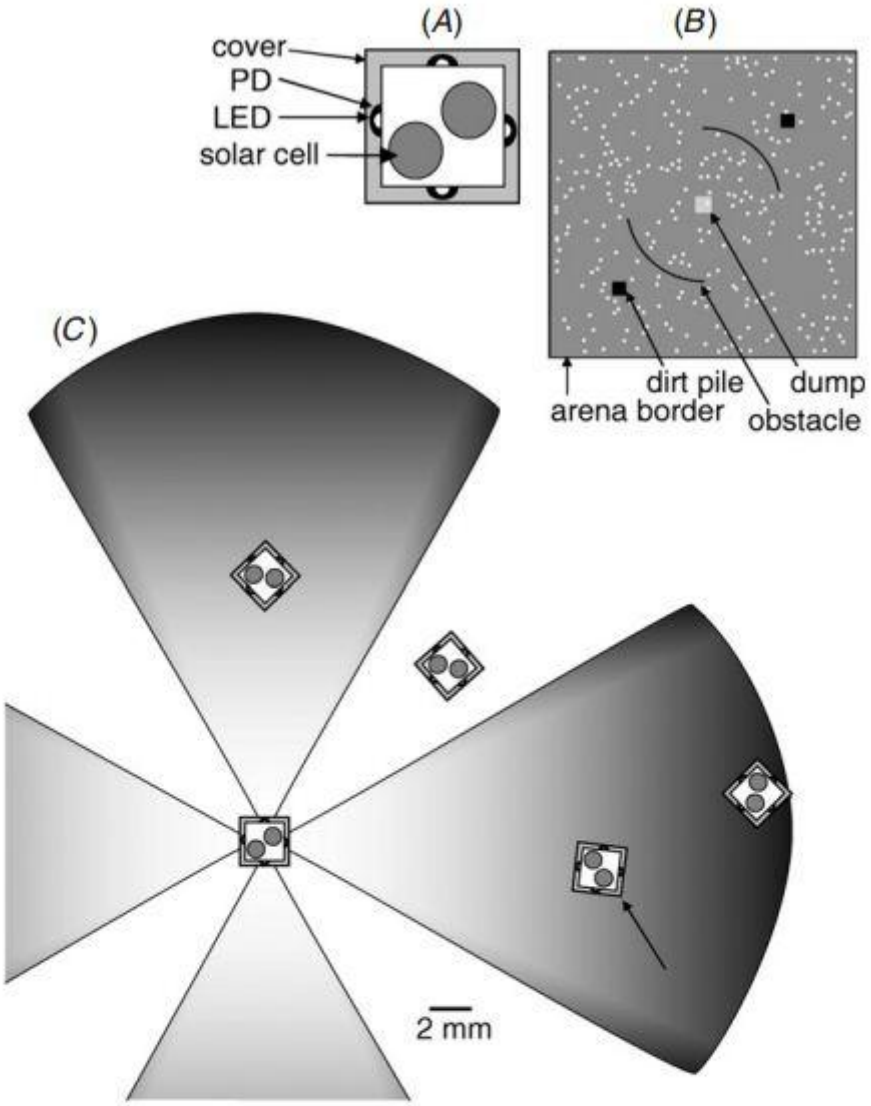

Figure 1. The appearance of the I-Swarm microrobot, the standard cleaning scenario and the geometry of the communication system. A bird's-eye view of an I-Swarm microrobot is given in (*A*). Two solar cells on top of the robot maintain energy supply provided by a constant light source. Under a cover (gray area) there are four photodiodes (PDs) and four light emitting diodes (LEDs) facing different directions. The standard cleaning scenario consists of two dirt piles (black squares) and a central dump (gray square) as shown in (*B*). Two large obstacles can be implemented in a cleaning scenario. Agents are shown as white dots. A schematic illustration of the signaling geometry of simulated agents is given in (*C*). In the given arrangement a supra-threshold signal is only detected by one (arrow) of four neighbors in the proximity of a signaling agent.

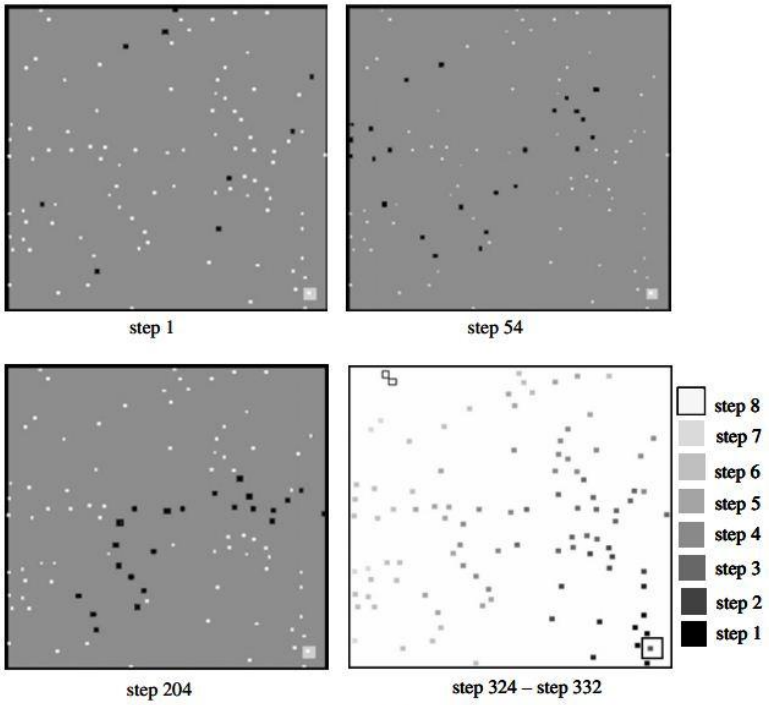

Figure 3. Establishment of synchronization waves (s-waves). In a simulation which allows us to study the establishment of s-waves immobile agents (dots) were randomly distributed in the arena at the beginning. Agents started at a random phase in their oscillator cycle and signal in the very last phase of their cycle (agents drawn in black). One agent exhibits a slightly faster oscillator cycle and is located at the lower right corner of the arena. After 50 simulation steps this agent triggers waves of synchronized signaling (s-waves) which spread out through the arena within only 8 simulation steps. These waves are generated in every oscillator cycle and were used as a guidance cue in the cleaning scenario.

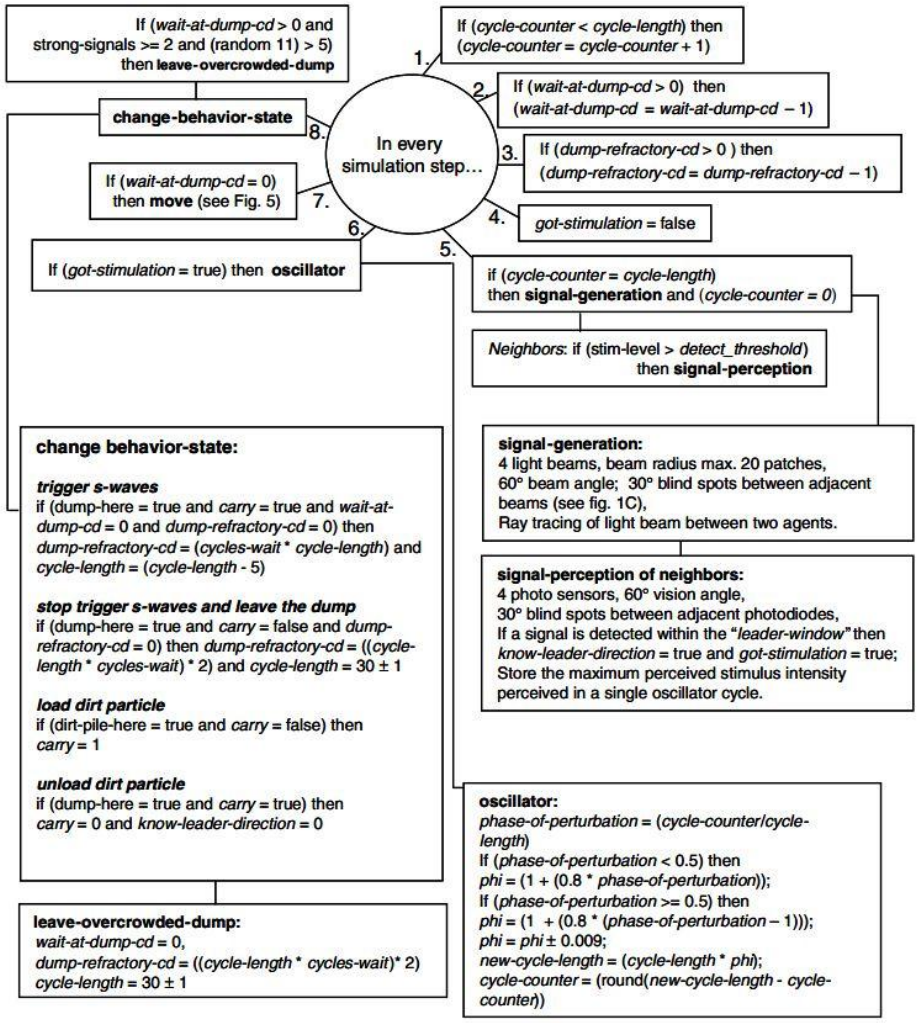

Figure 4. Instruction blocks executed by every agent in each simulation step. All agents execute eight logical program blocks in each simulation step. Agents could not execute the next block before all other agents finished the current block. ∗-cd refers to a variable holding a value that is count down by 1 in every simulation step.

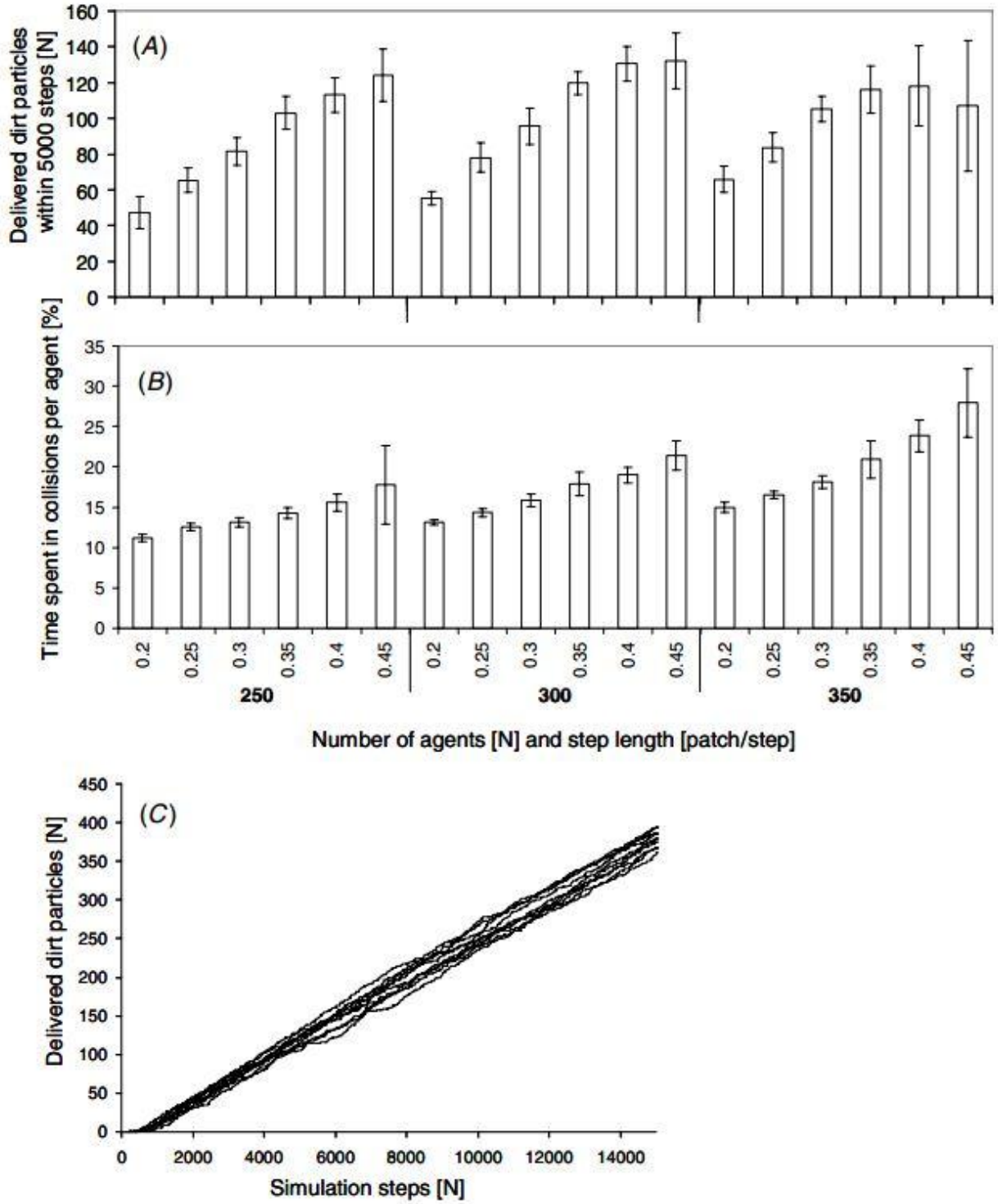

Figure 7. The influence of agent density and locomotion speed on swarm performance and agent interactions. In simulations of the SCS the mean quantity of delivered dirt particles which were counted at the dump within a simulation period of 5000 steps depends on the number of agents in the arena and the locomotion speed of agents (*A*). An increase of swarm performance was accompanied by an increase in the average time (simulations steps) each agent spent in escaping from collisions (*B*). (*C*) shows the temporal evolution of the number of delivered dirt particles collected within 12 long lasting simulation runs performed under optimal conditions. The agent density was 300 and the speed was 0.35 patches per step. The data shown in (*A*) and (*B*) represent the mean ± standard deviation obtained from 12 simulation runs.

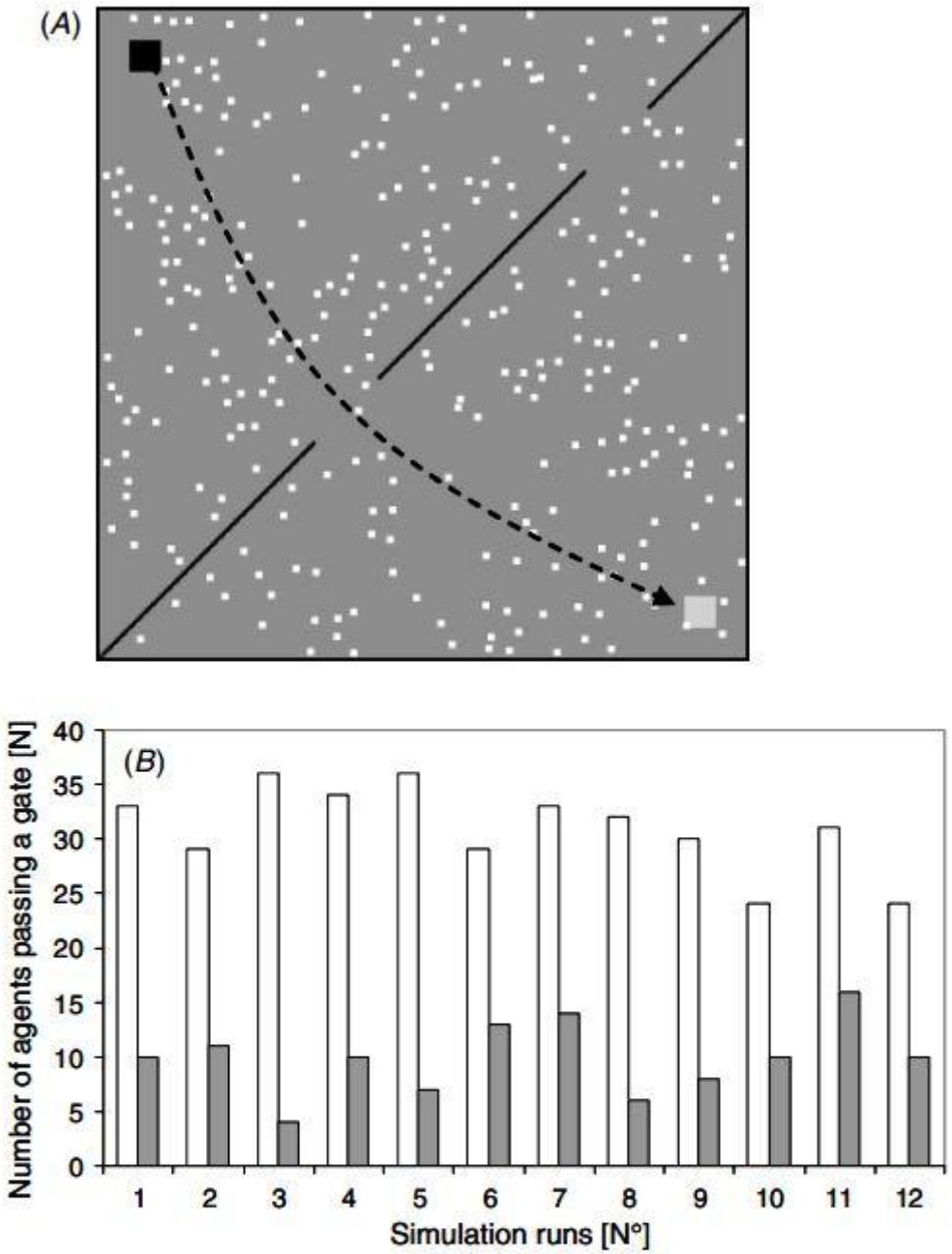

Figure 8. Collective decision making. Diagonally arranged obstacles create two asymmetrically arranged gates. One of these gates created a shorter (dotted arrow) path and the other gate created a longer path between the dirt pile (black square) and the dump (gray square) (*A*). The number of agents passing the gate belonging to the shorter path ((*B*), white bars) and the number of agents passing the gate belonging to the longer path ((*B*), gray bars) were counted in 12 simulation runs.

15. Chain Based Path Formation in Swarms of Robots

Nouyan S., Dorigo M.

In M. Dorigo and L. M. Gambardella and M. Birattari and A. Martinoli and R. Poli and T. Stutzle, editors, Proceedings of ANTS2006, pages 120-131, Springer Verlag, Berlin, Germany, 2006

Abstract. In this paper we analyse a previously introduced swarm intelligence control mechanism used for solving problems of robot path formation. We determine the impact of two probabilistic control parameters. In particular, the problem we consider consists in forming a path between two objects which an individual robot cannot perceive simultaneously.

Our experiments were conducted in simulation. We compare four different robot group sizes with up to 20 robots, and vary the difficulty of the task by considering five different distances between the objects which have to be connected by a path.

Our results show that the two investigated parameters have a strong impact on the behaviour of the overall system and that the optimal set of parameters is a function of group size and task difficulty. Additionally, we show that our system scales well with the number of robots.

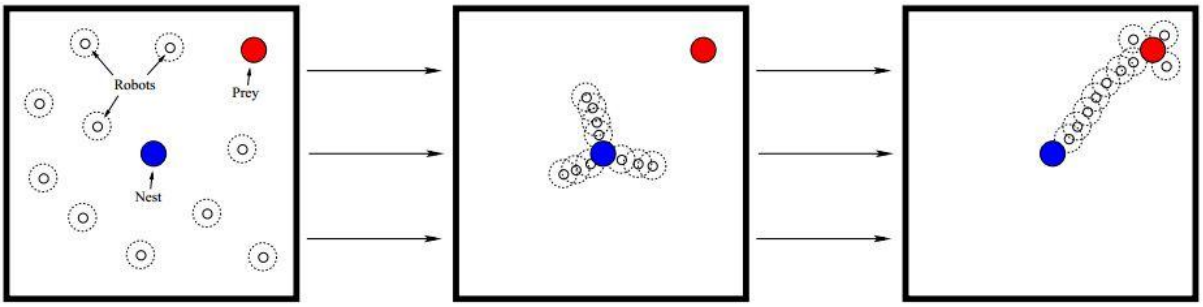

Fig. 1. (a) Initial situation. Robots are indicated by the small white circles. Their limited sensing range is indicated by dashed circles. The task is to form a path between the nest and the prey. (b) The robots search for the nest and once they find it they start self-organizing into randomly oriented chains. (c) When a chain perceives the prey a path is formed.

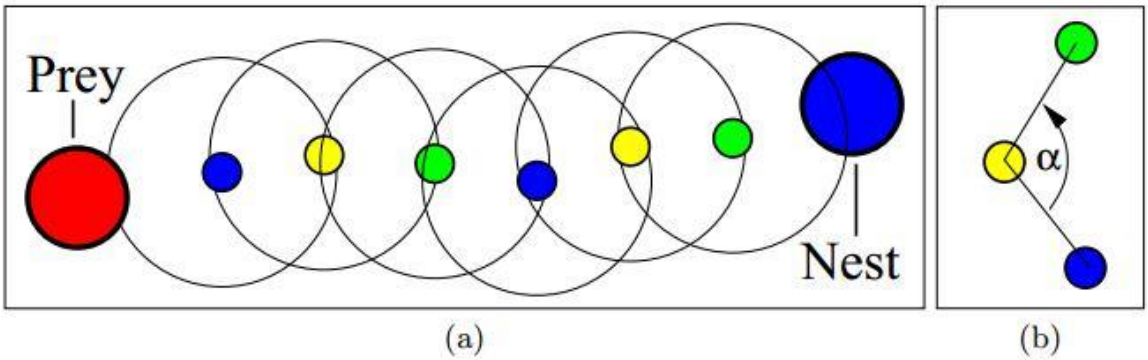

Fig. 3. (a) A chain with a cyclic directional pattern. The small circles represent robots that have formed a chain that connects a nest with a prey. Three colours are sufficient to give a directionality to the chain. The large circles surrounding the robots indicate their sensing range. (b) Alignment of a chain member. If the angle α is less than 120^o, the central chain member aligns with respect to its closest neighbours.

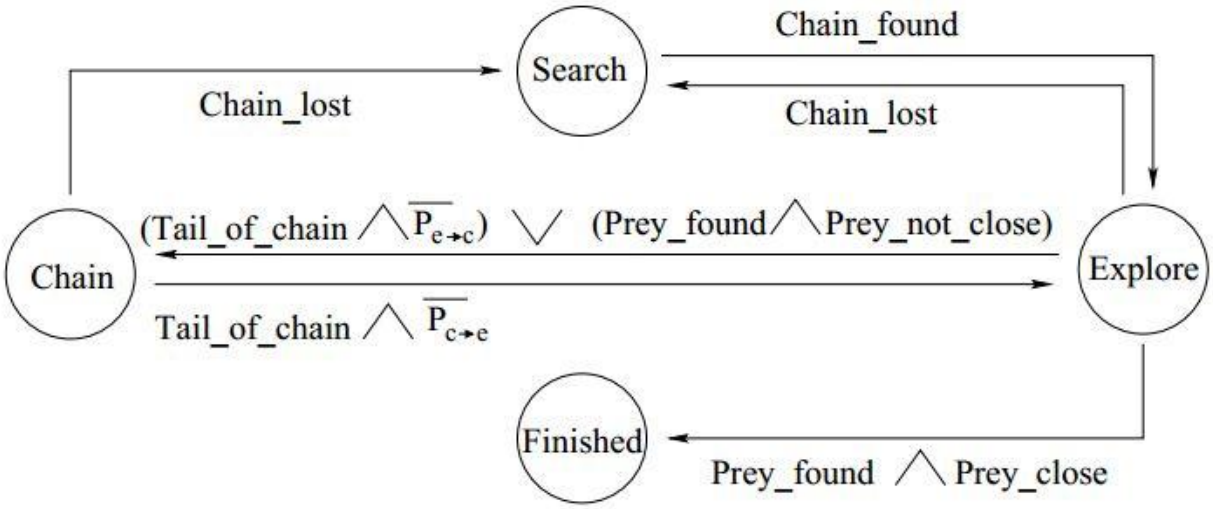

Fig. 4. . State diagram of the control. Each circle represents a state (i.e., a behaviour). Edges are labelled with the corresponding conditions that trigger a state transition. The initial state is the search state. $\overline{P_{e\to c}}$ (and $\overline{P_{c\to e}}$ respectively) is a boolean variable which is set to *true*, if $R \leq P_{e\to c}$ ($R \leq P_{c\to e}$), and to *false* otherwise, where R is a stochastic variable sampled from the uniform distribution in $[0, 1]$, and $P_{e\to c}$ ($P_{c\to e}$) is the probability per time step to aggregate to (disaggregate from) a chain.

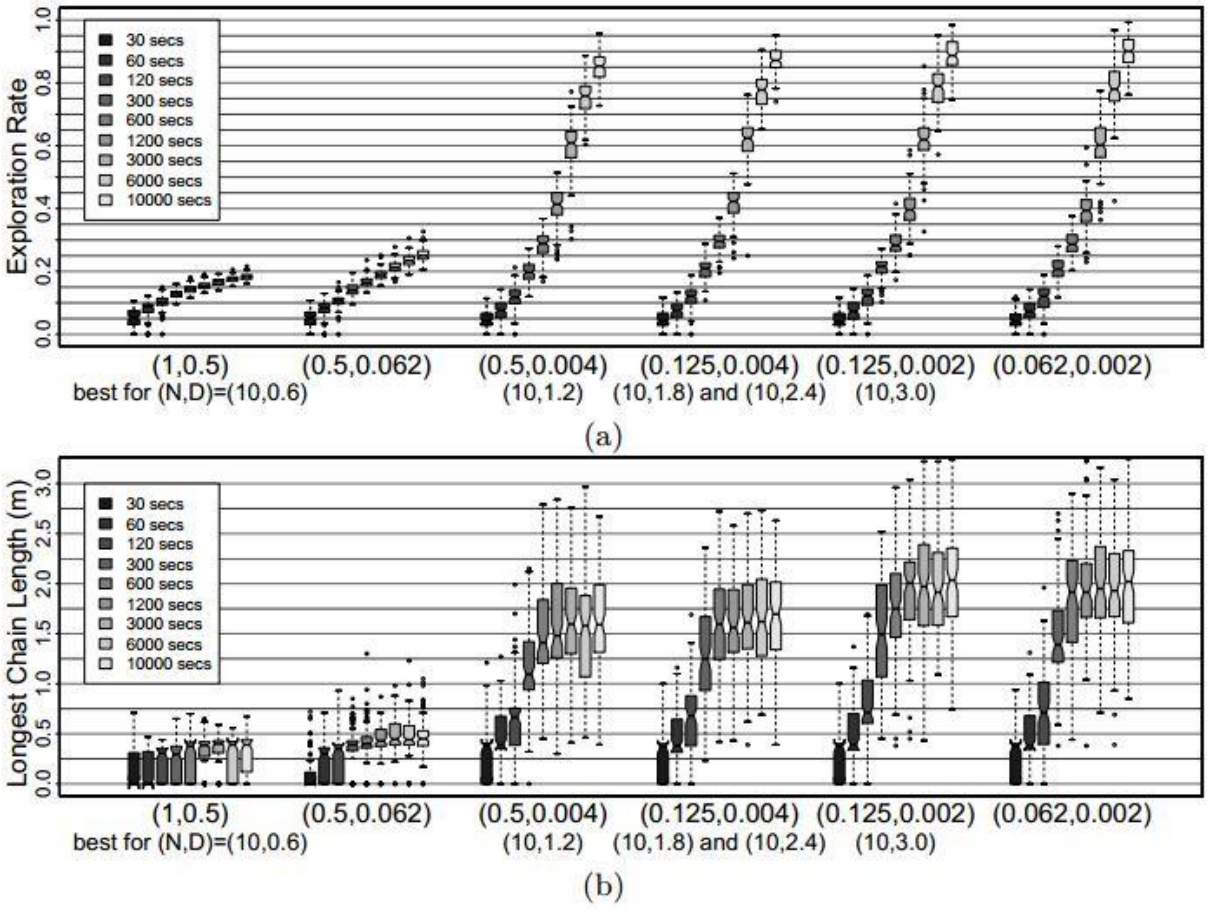

Fig. 6. For six selected parameter sets $(P_{e\to c}, P_{c\to e})$ (a) the exploration rate—defined as the percentage of the explored area within the arena—and (b) the length of the longest chain are displayed. The parameters were selected according to their success in the setups with $N = 10$ robots. The setup for which a parameter combination is most succesful is indicated below the probability values. Note that the combination $(P_{e\to c}, P_{c\to e}) = (0.125, 0.004)$ is the most successful one for both setups $(N, D) = (10, 1.8)$ and $(N, D) = (10, 2.4)$. Additionally, two parameter sets were selected by hand in order to allow for a better understanding of the overall effect of the probability values.

Сравнение состояния современной науки с предполагаемыми целями магистерской диссертации

Исследования в области групповой робототехники представлены достаточно широко, в свободном доступе находится обширное число материалов.

Тем не менее, исследований методов искусственного интеллекта на заранее не известном расположении роботов-целей на плоскости обнаружено не было. Также не было обнаружено в критериях эффективности различных алгоритмов суммарного угла поворота.